Title

Turbulence regimes in the nocturnal roughness sublayer: Interaction with deep convection and tree mortality in the Amazon

Authors

Mendonça, Anne CS
Dias-Júnior, Cléo Q
Acevedo, Otávio C
et al.

Publication Date

2023-08-01

DOI

10.1016/j.agrformet.2023.109526

Turbulence regimes in the nocturnal roughness sublayer: interaction with deep convection and tree mortality in the Amazon

Anne C. S. Mendonça[a], Cléo Q. Dias-Júnior[a,b,*], Otávio C. Acevedo[c], Raoni A. Santana[d], Felipe D. Costa[e], Robinson I. Negrón-Juarez[f], Antônio O. Manzi[g], Susan E. Trumbore[h], Daniel. M. Marra[h]

[a]*Amazonian National Research Institute (INPA-CLIAMB), Manaus, AM, Brazil*
[b]*Department of Physics, Federal Institute of Pará (IFPA), Belém, PA, Brazil*
[c]*Departamento de Física, Universidade Federal de Santa Maria, Santa Maria, RS, Brazil*
[d]*Institute of Engineering and Geosciences, Federal University of West Pará (UFOPA), Santarém, PA, Brazil*
[e]*Universidade Federal do Pampa, Alegrete, Brazil*
[f]*Lawrence Berkeley National Laboratory, Berkeley, CA, USA*
[g]*National Institute for Spatial Research (INPE), Cachoeira Paulista, SP, Brazil*
[h]*Biogeochemical Processes Department, Max Planck Institute for Biogeochemistry, Jena, Germany*

Abstract

We investigated the influence of seasonality and proximity to the forest canopy on nocturnal turbulence regimes in the roughness sublayer of a Central Amazon forest. Since convective systems of different scales are common in this region, we also analyzed the effect of extreme wind gusts (propagated from convective downdrafts) on the organization of the turbulence regimes, and their potential to cause the mortality of canopy trees. Our data include high-frequency winds, temperature and ozone concentration at different heights during the dry and wet seasons of 2014. In addition, we

*Corresponding Author
Email address: cleo.quaresma@ifpa.edu.br (Cléo Q. Dias-Júnior)

used critical wind-speed data derived from a tree-winching experiment and a modeling study conducted in the same study site. Two different turbulence regimes were identified at three heights above the canopy: a weakly stable (WS) and a very stable regime (VS). The threshold wind speeds that mark the transition between turbulence regimes were larger during the dry season and increased as a function of the height above the canopy. The turbulent fluxes of sensible heat and momentum during the WS accounted for 88% of the entire nighttime flux. Downdrafts occurred only in the WS and favored a fully coupled state of wind flow along the canopy profile. The destructive potential of winds was four times higher than on nights without downdrafts.
Keywords: Downdrafts, Extreme wind speed, Seasonality, Tropical forest, Turbulence regimes, Wind disturbance

---

1. Introduction

A growing number of observational and modeling studies show that the world's forests plays a key role in global climate (Malhi et al., 2002; Bonan, 2008; Alves et al., 2016) and emphasize its importance to the water, radiation and surface-energy balance. All these are affected by exchanges of mass (water vapor, carbon dioxide, methane, ozone, and a variety of gases and particles), heat (sensible and latent) and momentum between the forest and the atmosphere (Von Randow et al., 2004; Thomas and Foken, 2007; Knohl and Baldocchi, 2008; Gerken et al., 2016, among others). This near-surface boundary layer that is dynamically influenced by vegetation is called the roughness sublayer (RSL). Particularly at night, the transport efficiency decreases above the forest, which inhibits its penetration into the canopy (Cava et al., 2022) and leads to a decoupling between the sub- and upper canopy flows (Thomas et al., 2013; Freundorfer et al., 2019; Cava et al., 2022)

Assessments of turbulent flow are challenging in the nocturnal RSL, particularly during the occurrence of intense downdrafts that typically originate within a convective system (e.g. squall lines, super-cell and single-cell thunderstorms). Intense downdrafts can develop when cooled air from evaporating precipitation sinks rapidly towards the ground. Such events transport relatively cooler and drier air from the troposphere to the lower levels leading to changes in the thermodynamic and kinematic properties of the near-surface air mass (Wakimoto, 2015). These downdrafts can extend to the surface in the form of sudden variations in the values of the wind, pressure, turbulent fluxes and a drop in equivalent potential temperature (Garstang and Fitzjarrald, 1999; Betts et al., 2002; Dias-Júnior et al., 2017a; Melo et al., 2019; D'Oliveira et al., 2022). Such phenomena can gain an interesting physical interpretation when the turbulence is classified into distinct turbulent nocturnal regimes. In mid-latitude regions for example, Mahrt (1998) categorized turbulence as "weakly stable" and "very stable" to differentiate the conditions of sustained and non-sustained turbulence, respectively. Sun et al. (2012) classified the turbulence regimes as either weak or strong, according to the relationship between Turbulent Kinetic Energy (TKE) and wind speeds. Subsequently, such terms have been widely used to refer to the regimes.

The weakly stable regime follows Monin-Obukhov similarity theory, which is used in most atmospheric models for expressing the surface layer. On the other hand, the same is not true in the very stable regime (Mahrt, 1998, 2014). In general, numerical schemes such as those used in numerical weather prediction and atmospheric models reproduce the occurrence of both nocturnal turbulence regimes, but conditions that mark the transition between them depend on the parameterizations used to represent the eddy diffusivity (Costa et al., 2020). The transition between regimes is not universal, varying from one site to another. Such differences may be associated with local factors, for example by increased cloudiness (Acevedo and Fitzjarrald, 2003), surface roughness (Mahrt et al., 2013) and net nocturnal radiative loss (Sun et al., 2020; Acevedo et al., 2021).

Recent studies (Santos et al., 2016; Cava et al., 2022) have evidenced that the nature of the nocturnal-scalar exchange between the canopy and the overlying atmosphere is contrastingly dependent on the turbulence regime. While the weakly stable regime is dominated by turbulence, under very stable conditions a relatively larger fraction of the exchange is produced by non-turbulence motion with long time scales. This fact is particularly important for quantifying these fluxes since under very stable conditions the typical eddy-covariance methods might not properly capture the total exchange. Therefore, when assessing exchange patterns it is important to consider the following: Is the exchange seasonally dependent? If so, what seasonal processes affect the regimes? Is the nocturnal turbulence regime influenced by the frequency of convective downdrafts, which can affect the total canopy-atmosphere exchange of scalars? Therefore, experimental results obtained at different sites, such as in dense tropical forests, are essential to better understand the biosphere-atmosphere interaction and to improve existing knowledge on the nocturnal boundary layer.

From another perspective, in regions often covered by intense convective systems and convective cloud clusters, such as the Amazon region (Betts et al., 2002, 2003; Machado et al., 2002, 2004), the downdrafts may propagate strong downward wind gusts with high velocities (Fujita, 1985; Nelson, 1994; Garstang et al., 1998; Negrón-Juárez et al., 2010, 2017, 2018). When they reaches the surface, strong wind outflow with horizontal dimensions is propagated (Fujita, 1985; Garstang et al., 1998). These wind gusts can cause widespread tree damage and mortality through snapping and/or uprooting. These modes of tree mortality occur when the mechanical load caused by wind exceeds the resistance of the trunk or the root-soil anchorage (Nelson, 1994; Marra et al., 2014; Ribeiro et al., 2016).

The severity of damage/mortality caused by extreme wind events influences biomass balance and the functional composition of *terra-firme* forests in Central and Northwestern Amazon (Urquiza Muñoz et al., 2021; Negrón-Juárez et al., 2018; Marra et al., 2018, 2014). While some of the carbon contained in dead or damaged trees is decomposed and incorporated into the soil rather than directly emitted into the atmosphere (dos Santos et al., 2016), dead trees represent future CO_2 emissions (Chambers et al., 2004) and potentially methane (CH_4), which contributes to global warming. Using field data (Ribeiro et al., 2016) combined with static and dynamic biomechanical models, Peterson et al. (2019) estimated that wind speeds $> 10.75\ ms^{-1}$ are critical and can snap or uproot trees in *terra-firme* forests of Central Amazon.

Current knowledge about the effects of wind disturbances in the Amazon forest derives from studies that have quantified the spatial extent of these events using satellite imagery, in particular Landsat (Nelson, 1994;

Negrón-Juárez et al., 2010; Chambers et al., 2013; Espírito-Santo et al., 2014), or from post-perturbation forest inventories to assess associated tree damage/mortality and their effects on forest structure and diversity in subsequent years to decades (Marra et al., 2014, 2018; Schwartz et al., 2017; Silvério et al., 2019; Urquiza Muñoz et al., 2021). The estimated time to recover 90% of pre-disturbance biomass is up to 40 years (Marra et al., 2018) in the Central Amazon and 30 years in the northwestern Amazon (Urquiza Muñoz et al., 2021).

The goal of our study was to identify the existence of different nocturnal turbulence regimes above a *terra-firme* forest in the Central Amazon and their possible association with seasonality and proximity to the forest canopy. Furthermore, to assess the effect of extreme winds associated with convective downdrafts on the organization of turbulence regimes in the nocturnal RSL and the potential of observed winds to cause damage/mortality of canopy trees. We recognize that damaging winds and downdrafts in this region are also associated with convective storms and with fronts that can pass during the day, but that is beyond the scope of the current analysis. To our knowledge, this is the first assessment of the influence of extreme winds on turbulence regimes and of the potential of associated wind to promote tree damage/mortality. Apart from a better understanding of the processes of turbulent exchange between the biosphere and the atmosphere, especially in rainforests with dense canopies, our study provides insights into the vulnerability of Amazon forests to ongoing shifts on the intensity and frequency of convective storms resulting from climate change (Feng et al., 2023).

2. Material and methods

2.1. Study site and data acquisition

Our data were collected at the *Estação Experimental de Silvicultura Tropical* (EEST, also known as ZF2), Central Amazon, Brazil (Figure 1). The EEST is located about 60 km northwest of Manaus ($2^\circ\ 36'\ S$, $60^\circ\ 12'\ W$, 130 m $a.s.l.$) (Araújo et al., 2002) and is predominantly covered by old-growth *terra-firme* forest with closed canopy (e.g. 593 ± 28 trees ha^{-1}), dense understory and high tree-species diversity (Braga, 1979; Marra et al., 2014). Trees are relatively tall and slender (Oliveira et al., 2008; Ribeiro et al., 2016). The proportion of trees reaching the canopy increased with diameter at breast height (DBH): from 21% for trees 10-20 cm DBH, and 57% for 20-30 cm DBH, up to 100% for trees above 70 cm DBH (Araujo et al., 2020).

The topography at the study area comprises a mosaic of plateaus, slopes and valleys with elevation differences of about 50 m. The vegetation cover on the plateau and slope areas is composed by forest with height varying between 30 to 40 m, maximum surface area density of 0.35 m^2m^{-3}. In valley areas, the vegetation is smaller with heights from 15 to 25 m, but with significant surface area density more than the 0.35 m^2m^{-3} (Tóta et al., 2012). The average values of leaf area index for the local vegetation was 6.1 m^2m^{-2} (Marques Filho et al., 2005).

Oxisols rich in kaolinite clay dominate plateaus and the upper portions of slopes. The soils on slope bottoms and valleys are sandy and mixed with organic matter (Spodosol) (Telles et al., 2003). The mean annual temperature is 27 °C and mean annual rainfall was about 2365 mm for the period

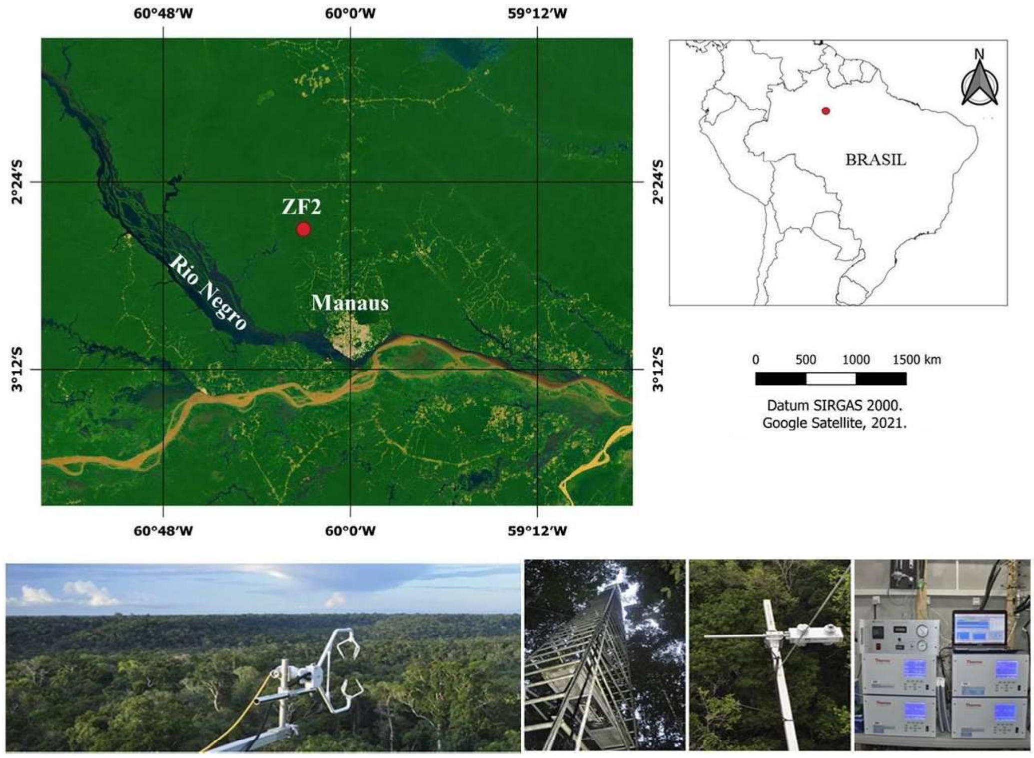

Figure 1: Study area at the *Estação Experimental de Silvicultura Tropical* (EEST) near Manaus, Brazil, and micrometeorological tower and sensors. (Top panel) Map of Brazil showing the study region. (Bottom left) A panoramic view of the forest and the employed 3D-sonic anemometer. (Bottom center left) Micrometeorological tower. (Bottom center right) Net radiometer. (Bottom right) Ozone analyzers.

between 1971 and 2000, with a distinct dry season between July and September (rainfall $< 100\ mm\ month^{-1}$) (Negrón-Juárez et al., 2017).

Our data were collected using sensors installed on a micrometeorological tower of 54 m height. We used the sonic virtual temperature (T) and wind components (u, v and w) measured at 10 different heights (i.e. 1.5, 7.0, 13.5, 18.4, 22.1, 24.5, 31.6, 34.9, 40.4 and 48.2 m above ground) by 3D-sonic anemometers (model CSAT3, Campbell Scientific Inc., Logan, UT, USA) at a rate of 20 Hz. For analyzing the vertical temperature gradient, we used thermo-hygrometer data from sensors (HMP45AC, Vaisala) installed at 35.5 m and 51 m height. These data were available at a 30 min resolution. Net radiation (R_N) was measured with a net-radiometer (model CNR1, Kipp & Zonen, Delft, Netherlands) installed at 39 m height. We used data from April 2014 to January 2015 collected in the course of the Green Ocean Amazon Experiment (GoAmazon). For more details about instruments and respective measurements, see Fuentes et al. (2016).

Ozone concentration (O_3) was measured continuously at 40 m height at a frequency of 1 Hz using an ultraviolet light absorbed gas analyzer (model 49i, Thermo Fisher Scientific Inc., Waltham, MA). For more details on ozone measurements see Gerken et al. (2016). Convective cloud coverage over the study site was assessed with GOES-13 (Geostationary Operational Environmental Satellites) satellite imagery data available at the Brazilian National Institute for Space Research (INPE) database (`http://satelite.cptec.inpe.br/acervo/`, accessed on 30 May 2021).

Our data were analyzed for two time periods: (i) 55 days in the wet season (from April to May) and (ii) 36 days during the dry season (from July to September). To avoid transitional periods, we used data from 2000 to 0500 local standard time (LST). The dry and wet seasons were characterized based on the seasonality of precipitation using the Global precipitation Mission (GPM) level-3 product ($mm\ h^{-1}$). Estimates were carried out using data downloaded from the website of National Aeronautics and Space Administration (NASA) (`https://giovanni.gsfc.nasa.gov`, accessed on 28 october 2020) for the period between 1st April and 31st December 2014.

Overall, we used a product of the Integrated Multi-satellitE Retrievals for GPM (IMERG) at a spatial resolution of 0.1° x 0.1° and at temporal resolution of 1 month (Final Run IMERGM v06). The IMERG algorithm combines information from the GPM satellite constellation and precipitation gauges. The system "final run" uses monthly gauge data to create research-level products.

Local estimates of critical wind-speed (CWS) were compiled from Peterson et al. (2019). According to these authors, the CWS is the wind speed necessary to generate a turning moment at the base of the trunk greater than or equal to the turning moment that results in tree failure. CWS were modeled based on critical turning moments measured locally in a winching experiment that included 60 trees from different species and varying sizes (Ribeiro et al., 2016). We considered CWS values estimated from a dynamic model (i.e. profile method) assuming that tree mortality associated with convective systems can create canopy gaps that contribute to increasing turbulence and wind propagation into the forest. In this model, tree spacing/density, leaf-area index and wind profiles are updated progressively after each tree failure (Peterson et al., 2019). The reported CWS ranged from 10.75 ms^{-1} to 34.5 ms^{-1}.

Before analyzing the micrometeorological, meteorological and profile data, we conducted the following quality control: (i) testing for record completeness and checking for the presence of error flags as proposed by Zahn et al. (2016) and (ii) detection of spikes and dropouts with eventual removal of corrupted/damaged data as suggested by Vickers and Mahrt (1997).

2.2. Turbulence regimes and flux estimates

In this study we examine the turbulence regimes at three heights. The first one was defined as near as possible to the top of the forest canopy (i.e. $\approx$ 35 m; Fuentes et al. (2016)), and the other two at the maximum heights where the sensors were installed on the tower (40 and 48 m, respectively). We focused only on the nighttime period (i.e., nocturnal boundary layer) because the diurnal relationship between wind speed and turbulence rarely deviates from linearity (not shown here), since typical daytime conditions at our study site are close to neutrality.

We used two methods for identifying the nocturnal turbulence regimes. The method proposed by Sun et al. (2012, 2016) considers the possibility of external agents (e.g. convective clouds) acting on the atmospheric boundary layer and disturbing its turbulent fields (Garstang et al., 1998; Garstang and Fitzjarrald, 1999; Betts et al., 2002; Dias-Júnior et al., 2017a). Sun's method accounts for the average relationship between the turbulent velocity scale (V_{TKE}) and the mean horizontal wind speed (V). Where $V_{TKE} = \sqrt{TKE} = [0.5({\sigma_u}^2+{\sigma_v}^2+{\sigma_w}^2)]^{1/2}$ and $V = \sqrt{u^2+v^2}$, in which u, v and w are zonal, meridional and vertical wind components, σ represents the standard deviation of each variable and TKE represents the Turbulent Kinetic Energy. Sun's method identifies the wind speed threshold value (V_L) from the slope change of a straight line around which the data are clustered. For this, we performed a segmented linear regression and selected the V_L with the best coefficient of determination (R^2). In this case, turbulence is compared at a given level with the wind speed at that level.

The second method, reported by Acevedo et al. (2016) is based on the sign inversion of the vertical gradient of V_{TKE} (ΔV_{TKE}). This procedure accounts for the relationship between V_{TKE} and V, but in contrast to Sun's method, turbulence is examined at all levels in terms of the wind speeds at a fixed reference level. When classified by the V at a reference level, the wind speed crossover threshold (V_T) lies where the average ΔV_{TKE} reverses sign for the entire tower layer. This change occurs because in very stable regime the V_{TKE} increase with height and the importance of low-frequency (sub mesoscale fluctuations) phenomena at higher levels contributes to this pattern. In weakly stable regime, on the other hand, the classical pattern of decreasing turbulence with height is dominant. Therefore, the parameters V_L and V_T are the wind speed values that determine the change from very stable (decoupled boundary layer) to weakly stable regime (the classical boundary layer coupled to the surface). Here, we assumed ΔV_{TKE} as the difference between 48 m and 35 m.

Fluxes were estimated by the Eddy Covariance method. We calculated the turbulent fluxes of sensible heat as $H = \rho c_p \overline{\theta' w'}$ and momentum as $\tau = \rho(\overline{u'w'}^2 + \overline{v'w'}^2)^{1/2}$, where ρ is the density of air (assumed to be 1.225 kgm^{-3}) and c_p is the specific heat of air at a constant pressure. The variables θ' and w', represent the fluctuations of virtual temperature (°C) and vertical wind speed (ms^{-1}), respectively. As suggested by Sun et al. (2002) and Vickers et al. (2010), we used mean values over 5 min intervals for all the different statistical moments of the turbulence.

To investigate statistical differences between the very stable and weakly stable regimes, we first used the Mann Whitney U-test considering the identified regimes as grouping variables. Therefore, six tests were performed, one at each height (48 m, 40 m and 35 m) and for the dry and wet seasons. In a second analysis, we applied a factorial analysis of variance (ANOVA) followed by Tukey tests to assess the effects of the interaction between the seasons, heights and turbulence regimes on observed patterns of atmospheric turbulence. Here we use V_{TKE} as dependent variable. For all tests we considered a significance level of 5% and used the software Matlab and Jamovi for data processing and analysis.

In this work V_{TKE} was only used in the analysis of the transition of turbulence regimes, but not as an indicator of the tree damage/mortality. To assess the potential of extreme wind gusts as a mechanism of tree damage/mortality, we compared the CWS data available for our study site and the maximum wind speed observed within our study period, as detailed in section 2.4.

2.3. Identification of convective cloud downdrafts

Previous studies have demonstrated that convective downdrafts transport air with high O_3 concentrations and lower T (cold pool) rapidly from the lower-middle troposphere to the surface (Betts et al., 2002; Gerken et al., 2016; Dias-Júnior et al., 2017a; Bezerra et al., 2021).

It is known that in environments with high moisture and strong convection such as in the Amazon, the equivalent potential temperature (θ_e) is also important under unstable atmospheric conditions. Since θ_e changes as a function of moisture (through mixing ratio) and temperature, the downward transport of cold and dry air leads to an important decrease of θ_e (Garstang and Fitzjarrald, 1999; Betts et al., 2002). However, moisture data were not available for our study site. Alternatively, we used virtual temperatures.

The identification of convective cloud downdrafts in our study was performed using a two-step procedure. We first analyzed the time series of horizontal wind speed, air temperature and surface concentration of O_3 to investigate atmospheric dynamics and the occurrence of gust fronts associated with convective clouds. For this analysis, we averaged data at 48 m (V and T) and 40 m (O_3) height for 5-minute intervals. The data series were mapped by an algorithm that identifies a subtle increase of O_3 concentrations of at least 3 parts per billion (ppb), and a simultaneous decrease of T values of 2 °C within a 1h time window of respective events (Gerken et al., 2016; Dias-Júnior et al., 2017a). During these events, the highest horizontal wind speed registered within one second interval and the five minutes average comprising such an interval were retained. False detections were manually identified and removed. In the next step, GOES-13 imagery were visually inspected for the presence of convective clouds over the study site. Here, we only considered images acquired on days for which abrupt changes in weather variables were detected as described in the previous step. We analyzed the effect of downdrafts associated with turbulence regimes by checking the relationship between V_{TKE} and V. Here, we assumed the minimum and maximum V values to determine the start and end time of respective wind gusts.

2.4. Extreme winds as a mechanism of tree mortality

To assess the potential of extreme wind gusts as a mechanism of tree damage/mortality, we compared the CWS data and the maximum wind speed (V_o) measured by our anemometers. The V_o is the maximum horizontal wind speeds (or extremes winds) measured at 5 min time-intervals at 48 m height.

These data were analyzed for the different seasons (dry and wet).

Since downdrafts can last from few seconds to (rarely) minutes, we calculated V_o at two other time intervals: 1-minute and 30-seconds windows. To check if V_o differs with the size of time-intervals, we compared computed values (response variable) using ANOVA of repeated measures. Subsequently, we executed an ANOVA to verify potential variations of V_o as a function of seasonality.

3. Results

3.1. Turbulence regimes in the nocturnal boundary layer

We found a positive relationship between V_{TKE} and V for both dry and wet seasons, and a clear distinction between the two turbulence regimes (Figure 2). For events classified as weak turbulence (very stable regime), V_{TKE} increased less than V as indicated by a smaller slope. As V reached a threshold value (V_L), turbulence changed from weak to strong (weakly stable regime) as indicated by a larger increase of V_{TKE} as a function of V and larger slope. V_L increased nonlinearly with the distance from the forest canopy in both seasons. The observed values of V_L at 35 m and 48 m were near 0.7 and 2.3 ms^{-1} (dry) and 0.5 and 1.9 ms^{-1} (wet), respectively. These results are in agreement with previous studies that found that V_L increases nearly logarithmically with height (Sun et al., 2012; Acevedo et al., 2016).

Although the observed increase of V_L with height supports previous research on non-vegetated surfaces, the thresholds identified at 35 m in our study site were significantly smaller than those observed at a pasture area at the Federal University of Santa Maria (in south Brazil) (V_L of 3.0 ms^{-1} at

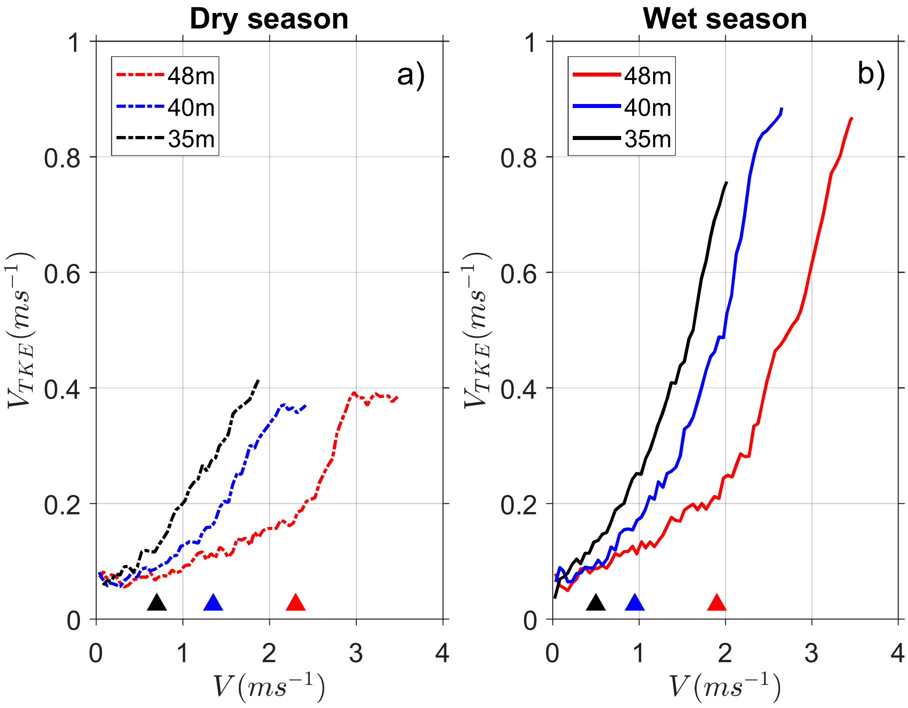

Figure 2: Relationship between turbulence velocity scale (V_{TKE}) and mean wind speed (V) at different heights in the (a) dry and (b) wet season during the nighttime at the EEST, Manaus, Central Amazon. Triangles indicate the threshold wind speed (V_L) at which the very stable changed to weakly stable regime.

30 m height) (Acevedo et al., 2021) and at project FLOSS II (Fluxes over Snow Surfaces) conducted in Colorado (US) (V_L of 5.3 ms^{-1} at 30 m height) (Acevedo et al., 2016). Such differences show that the structure and roughness of dense forests influence the change of the turbulence regime. For a proper comparison we considered the observation level with respect to the zero plane displacement height (d). We used d=31.5 m based on estimates provided by Viswanadham et al. (1990) and Chor et al. (2017) for central Amazon, in which d=0.88h and d=0.9h, respectively, where h is the canopy

height (35 m at our study site). Doing that, the V_L values found at 35 m (z-d = 3.5 m) in both seasons are smaller than the value of 2.04 ms^{-1} found at 2 m in FLOSS II (Acevedo et al., 2016) and that of 1.5 ms^{-1} found at 1.5 m in the CASES-99 (experiment carried out in southeast Kansas, US) (Sun et al., 2012). Similarly, the V_L found for both seasons at the EEST at 48 m (z-d=16.5 m) are smaller than those at 15 m in FLOSS (5.04 ms^{-1}) and at 10 m in CASES-99 (4.5 ms^{-1}). The V_L found at 48 m at EEST site in the wet season is also smaller than the value reported by Acevedo et al. (2021) at 14 m in Santa Maria (2.2 ms^{-1}). Still, this value is close to that we found during the dry season at the EEST. In general, the V_L values between turbulence regimes was smaller at the EEST site than that reported in previous studies at similar heights, even when the zero-plane displacement height is taken into account. This relates to V_L being generally smaller above rough surfaces compared to smooth surfaces (Mahrt et al., 2013; Vignon et al., 2017; Guerra et al., 2018), a simple consequence of turbulent mixing being larger above a rough surface than above a smooth one at a same mean wind speed.

From the nighttime turbulence regimes identified at 48 m height, around 77% (dry) and 65% (wet) of them were associated with very stable regime. In contrast, weakly stable regime corresponded to 23% (dry) and 35% (wet) of the events. Furthermore, V_L was larger during the dry season than in the wet season at the three investigated heights (Figure 2 and Table 1). This result is in agreement with Acevedo et al. (2021), who showed that V_L increases linearly with net radiative loss at the surface at three mid-latitude sites. According to these authors, the fully turbulence regime occurs when the mean wind speed is large enough to support heat fluxes capable of transferring back to the surface part of the energy lost radiatively. Therefore, such a minimum heat flux and corresponding minimum wind speeds must be larger when the net radiative loss is also larger. The relationship between V_L and R_N is further discussed in Section 4.

Table 1: Wind speed threshold (V_L) at studied heights for the dry and wet seasons at the EEST, Manaus, Central Amazon.

Season	V_L at 48m (ms^{-1})	V_L at 40m (ms^{-1})	V_L at 35m (ms^{-1})
Dry	2.3	1.35	0.7
Wet	1.9	0.95	0.5

We also identified the transition between regimes as a function of V at 35 m, for which the ΔV_{TKE} reverses sign for both dry and wet seasons (Acevedo et al., 2021). Figure 3 show that the V_{TKE} increased with height for weak winds in both seasons. When V at 35 m exceeds a sharp threshold, this pattern is reversed, so that V_{TKE} decreases with height under sufficiently strong winds. Such a threshold was approximately 0.65 ms^{-1} and 0.50 ms^{-1} for the dry and wet seasons, respectively. However, when the same analysis is performed in terms of V at 48 m (Figure 4), there was no gradient reversal and V_{TKE} decreased with height for all observed wind speeds.

These findings suggest that the relationship between V and V_{TKE} at the different heights is not trivial and may be associated with the occurrence of phenomena such as low-level jets and density currents (Greco et al., 1992; Dias-Júnior et al., 2017b; Corrêa et al., 2021). When the wind speeds are weak at higher levels, the wind profile is often distorted and maximum values can occur near the surface (Acevedo et al., 2016).

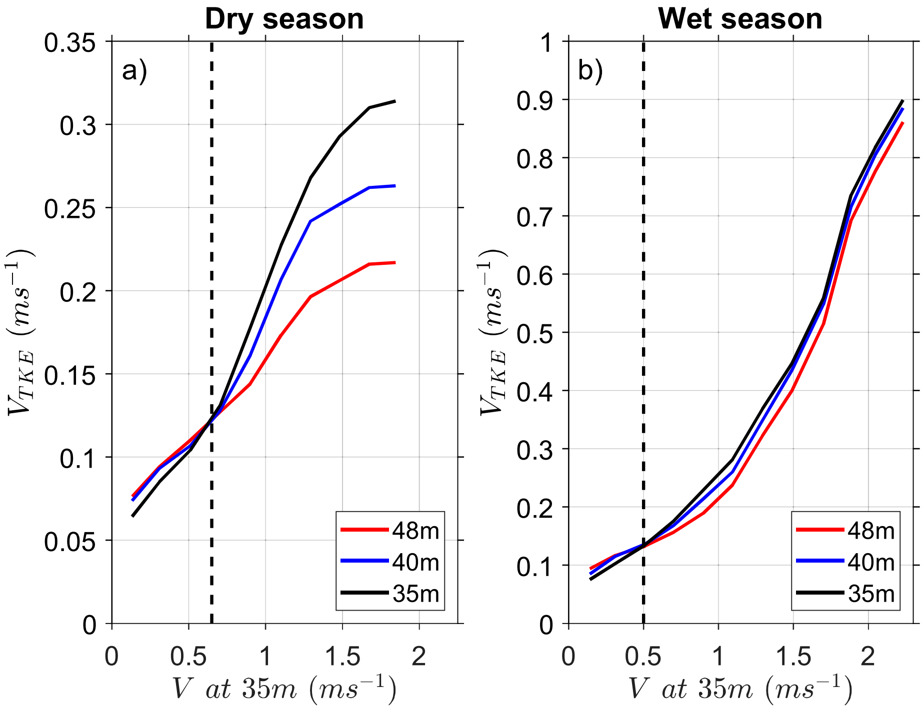

Figure 3: Turbulence velocity scale (V_{TKE}) as a function of the mean wind speed (V) at 35 m during the nighttime at the EEST, Manaus, Central Amazon. The solid lines are V_{TKE} at different heights in the (a) dry and (b) wet season. Black vertical dashed line indicates when V_{TKE} reverses its sign and exceeds the crossover threshold (V_T) at which the very stable changed to weakly stable regime

The V_T values identified by the vertical gradient method at 35 m height during the dry (0.65 ms^{-1}) and wet (0.50 ms^{-1}) seasons were similar to the V_L values obtained with Sun's method. This result corroborates the existence of nighttime turbulence regimes at the EEST during the two seasons. As the values of V_T and V_L were similar, hereafter we used the values of V_L as an indication for changes of turbulence regimes, since it was possible to identify it at all heights investigated here.

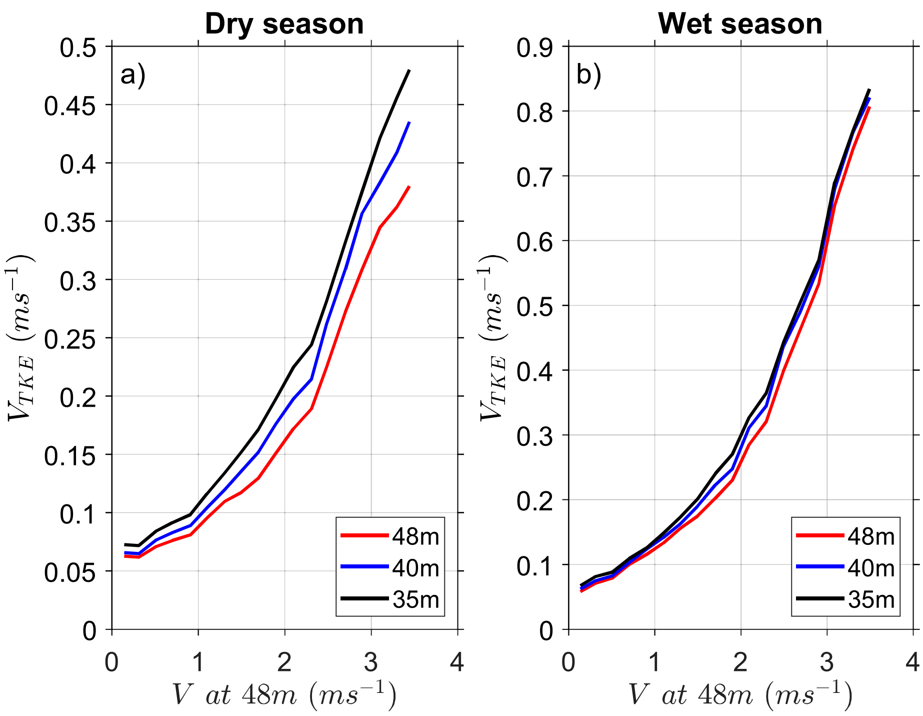

Figure 4: Turbulence velocity scale (V_{TKE}) as a function of the mean wind speed (V) at 48 m during the nighttime at the EEST, Manaus, Central Amazon. The solid lines are V_{TKE} at different heights in the (a) dry and (b) wet season

Our results evidenced the existence of different nocturnal turbulence regimes in the *terra-firme* Amazon forests. Moreover, they indicated that turbulence intensity decreased with the proximity to the canopy (Figure 5a). V_{TKE} during weakly stable regime was larger than in the very stable regime (Figure 5b). Overall, the wet season had larger values of V_{TKE} than the dry season (Figure 5c).

These larger values of V_{TKE} in the wet season are likely associated with a lower wind speed threshold between regimes in the wet season (Figure 2). Since the threshold is smaller, it is plausible considering that it is easier to overcome this threshold and establish "large" V_{TKE} in this case. Another reason that could result in larger values of V_{TKE} in the wet season would be simply because the wet season has higher wind speeds values than the dry season. Nonetheless, this was not the case, as can be seen in Figure 5d-f. Our result may be related to other factors, such as radiative loss, thermal gradient, among others.

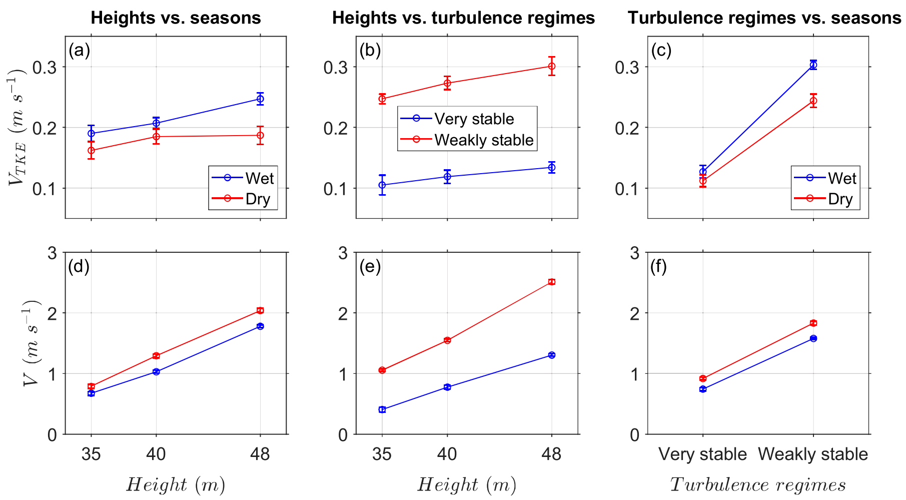

Figure 5: Turbulence velocity scale (V_{TKE}) and mean wind speed (V) as a function of (a,d) heights vs. seasons, (b,e) heights vs. turbulence regimes and (c,f) turbulence regimes vs. seasons during nighttime at the EEST, Manaus, Central Amazon. Legend: circles and vertical bars indicate mean values and the 95% confidence intervals, respectively

3.2. Turbulent fluxes in the nocturnal boundary layer

We investigated the differences between the turbulent fluxes during the occurrence of very stable and weakly stable regimes, and found an interesting relationship between V and the sensible heat (H), and momentum (τ) fluxes at 35 m height during both seasons. Bins of V each 0.2 ms^{-1} were used to calculate the average values and standard deviations of the fluxes. H values (Fig. 6a and Fig. 6b) changed in response to the turbulence shifting from the weak to the strong in both seasons (Table 2). On average, the H flux in the weakly stable regime corresponded to about 88% of the total H observed in both seasons. Our findings corroborate those of previous research conducted in Eastern Amazon (Dias-Júnior et al., 2017b). Importantly, H values were more intense during the dry season ($p = 0.001$). This result is possibly associated to larger net radiative loss due to reduced cloud cover and atmospheric column water vapor load (Collow and Miller, 2016), which leads to less longwave radiation reaching the canopy.

Table 2: Mean values ($\pm$ 95% confidence interval) of sensible heat flux (H) and momentum flux (τ) for the dry and wet seasons at the EEST, Central Amazon, Brazil.

Turbulence regimes	H Dry (Wm^{-2})	H Wet (Wm^{-2})	τ Dry (10^{-2}) (Nm^{-2})	τ Wet (10^{-2}) (Nm^{-2})
Very stable	-1.8 $\pm$2.5	-1.3 $\pm$2.0	-0.3 $\pm$ 0.4	-0.5 $\pm$ 0.6
Weakly stable	-13.4 $\pm$ 17	-9.8 $\pm$ 9.6	-2.3 $\pm$ 3.0	-4.1 $\pm$ 5.4

The τ fluxes showed a similar behavior to that of H, in which the flux in the weakly stable regime was larger than in the very stable regime ($p \leq 0.001$), and reached on average 89% of the total τ flux in each season (Fig. 6c and Fig. 6d). Such variations may be related to atmospheric stability conditions. The wet season is less stable (on average), that is, the strong turbulence events (i.e. weakly stable regime) occurs more frequently and, consequently, the momentum fluxes are greater. Overall, the weakly stable regime contributed more significantly to sensible heat and momentum fluxes than the very stable regime (Table 2), in both seasons.

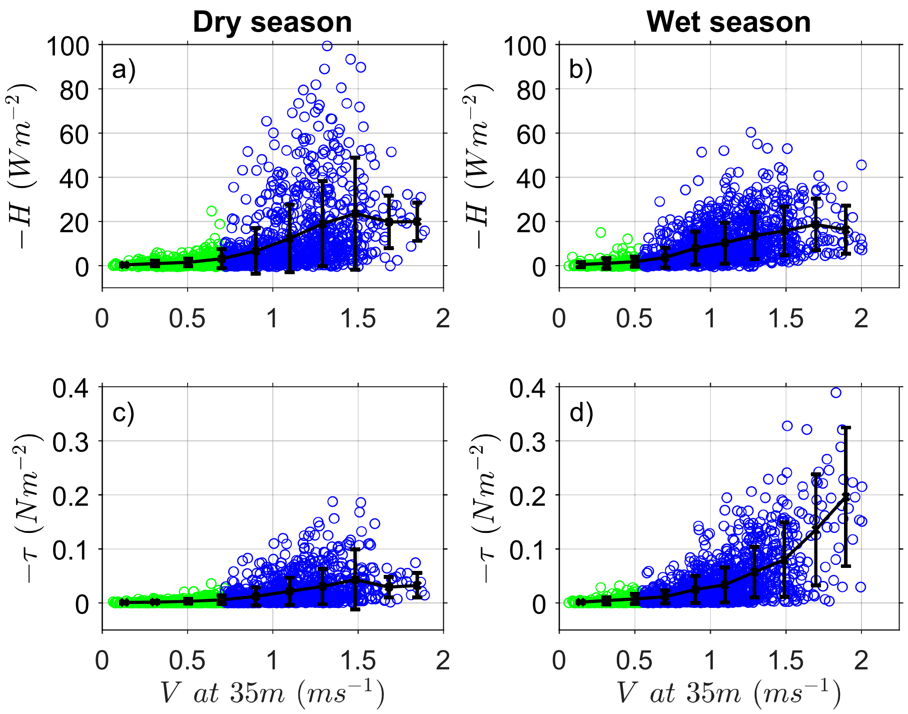

Figure 6: Mean and standard deviation of sensible heat flux (H) and momentum flux (τ) as a function of the wind speed (V) at 35 m during nighttime at the EEST, Manaus, Central Amazon. The left and right panels indicate the dry and wet season, respectively. Green and blue circles indicate the very stable and weakly stable regimes, respectively.

3.3. Relationship between deep convection and nocturnal turbulence regimes

During the night of 06 August 2014 and 12 April 2014, gust fronts from downdrafts reached the tower around 2110 LST (dry season) and 2325 LST (wet season), respectively (Figure 7). These events were evidenced from observations of (i) decreasing T (around 2 °C at both seasons) and (ii) simultaneous increasing O_3 of approximately 12 ppb (dry) and 15 ppb (wet). The pre-gust measurements of V ($\approx 2\ ms^{-1}$) were similar in both nights (Fig. 7c and Fig. 7g). However, V reached maximums of 7.5 (dry) and 15 ms^{-1} (wet) during the observed downdrafts. At this time, the standard deviation of wind vertical velocity (σ_w) increased substantially (Fig. 7d and Fig. 7h). As the surface cools and uncouples the boundary layer from the above troposphere, the near-surface O_3 values are low (3-5 ppb). This pattern allows for a clear recognition of night downdrafts transporting air with higher ozone and lower temperature to the surface. We observed this pattern on other nights and identified 16 downdrafts (eight different nights in each season) over the studied period. Overall, these events occurred between 2000 LST and 2300 LST. Finally, the GOES-13 imagery indicates the existence of cloudiness at the times of the events (Figure 8) and also on the other 16 nights that we studied here.

These results support previous studies, such as that by Betts et al. (2002) who found that nighttime convective downdrafts coupled the surface to the lower troposphere and transported down air with larger O_3 and lower equivalent potential temperature. Dias-Júnior et al. (2017a) also reported that the downdrafts produce O_3 enhancement events and an increase in V values, in addition to the occurrence of air divergence during the horizontal propagation of density currents.

We observed that all downdrafts happened during or after the transition to the weakly stable regime (Figure 9). This pattern evidenced that downdrafts may influence the turbulence characteristics near the surface since they are associated with a weakly stable regime (strong turbulence). However,

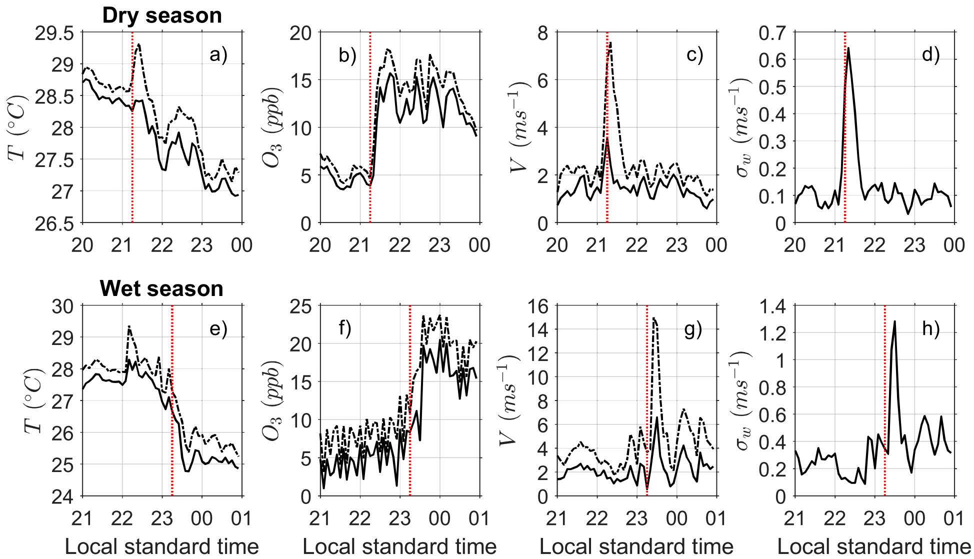

Figure 7: Times series of key variables used to identify downdrafts at the EEST, Central Amazon, Brazil. The upper and bottom panels show the downdrafts from 06 August 2014 and 12 April 2014, respectively. Legend: virtual temperature (T), ozone (O_3), horizontal wind speed (V) and standard deviation of wind vertical velocity (σ_w). Solid and dashed lines indicate the mean and maximum values, respectively. Vertical red-dotted lines indicate the starting time of downdrafts.

weakly stable regime was not represented completely by these events, which suggest that the strong turbulence may be associated with the occurrence of other phenomena. Similar results were previously reported for Central Amazon by Bezerra et al. (2021), who observed that downdrafts generated by a squall line occurred only during the strong turbulence regime.

3.4. Extreme winds as a mechanism of tree mortality

During the weakly stable regime associated with nocturnal downdraft events, the speeds and thus destructive potential of winds varied between

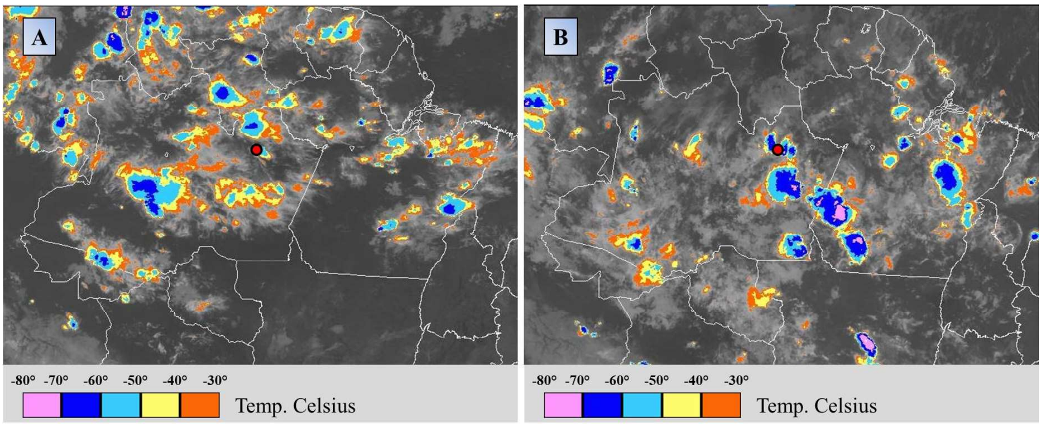

Figure 8: GOES 13 imagery for (a) 07 August 2014 at 0100 UTC and (b) 13 April 2014 at 0300 UTC when downdrafts reached the micrometeorology tower at the EEST (red dot), Central Amazon, Brazil.

seasons. The greatest wind speeds were identified during the wet season (V_o= 14.96 ms^{-1}). This value was approximately four times higher than on nights without downdrafts, and exceed the CWS of three out of the studied trees by Peterson et al. (2019). In contrast, maximum wind speeds in the nocturnal period of the dry season (V_o= 7.57 ms^{-1}) did not exceed the CWS of the studied trees.

Here we did not assess the direct effect of high wind-speeds on trees, but rather evaluated the destructive potential of these based on observational data acquired at the same study site. Importantly, the occurrence of excessive wind speeds does not necessarily result in trees damage and mortality. Further studies are needed to understand the link between wind speeds, canopy structure and tree motion in these diverse forests. Still, the strong dissipation of air to layers below the forest canopy (presented in Section 4) are rarely observed in the absence of downdrafts. Therefore, the wind gusts

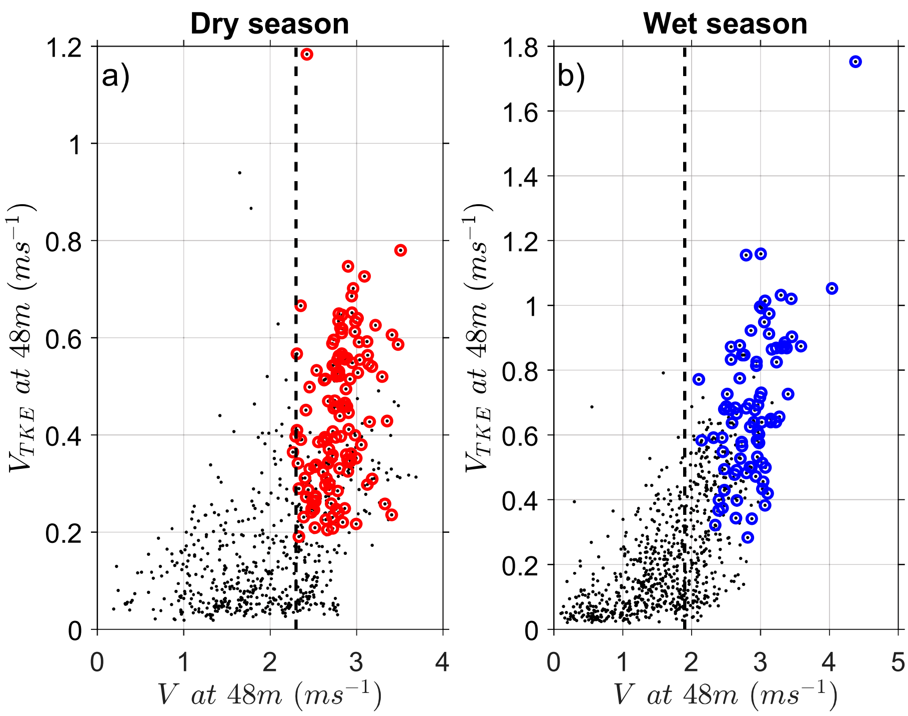

Figure 9: Turbulence velocity scale (V_{TKE}) as a function of the mean wind speed (V) measured at 48 m in the (a) dry and (b) wet season during nighttime at the EEST, Manaus, Central Amazon. The dots correspond to mean values calculated over 5-min periods. Thick circles indicate the range of occurrence of the downdrafts. Vertical black-dashed lines mark the threshold wind speed (V_L) at which the very stable changed to weakly stable regime.

described in our study not only reached extreme speeds but also penetrated the forest canopy, and had the potential to cause damage and mortality of trees of different sizes, both directly and indirectly.

The mean V_o values varied significantly between the analyzed time-intervals ($p \leq 0.001$, Fig. 10a). As expected, the values were higher for the 30 seconds interval (5.97 ± 2.85 ms^{-1}, mean $\pm$ 95% confidence interval). For the 1 min and 5 min intervals, V_o was 5.35 ± 2.68 ms^{-1} and 3.63 ± 2.45 ms^{-1}, respectively. Results from subsequent ANOVA showed that the interaction between seasons and time intervals was significant ($p \leq 0.001$, Fig. 10b). Post-hoc Tukey tests showed that observed variations in V_o were not significantly different between seasons at both 1 min ($p = 0.057$) and 5 min ($p = 1.000$) intervals. Nonetheless, V_o varied as a function of seasonality for our shorter time interval (i.e. 30 seconds). These result shows that for extreme wind gusts that may last a few seconds such as those causing tree damage and mortality in the Amazon, our 30 second interval is likely too large and may have underestimated maximum V_o values.

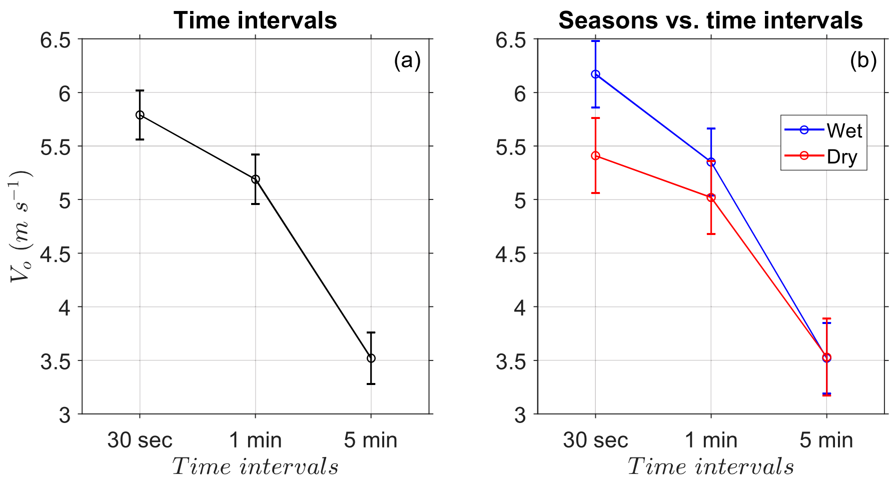

Figure 10: Observed wind speed (V_o) as a function of the (a) three time intervals and (b) seasons vs. time intervals at the EEST, Manaus, Central Amazon. Legend: circles and vertical bars indicate mean values and the 95% confidence intervals, respectively.

Although daytime patterns were not a focal aspect in our study, wind speed reached the highest values (up to 22 ms^{-1}) during this period, in the dry season. In contrast to the relatively low destructive potential of nocturnal winds, this value could topple 73% of trees previously investigated in our study site (Ribeiro et al., 2016; Peterson et al., 2019). These observations reinforce the importance of extreme wind as a major natural mechanism of tree damage and mortality in these forests (Nelson, 1994; Chambers et al., 2009, 2013; Negrón-Juárez et al., 2017, 2018; Marra et al., 2018).

In fact, a higher destructive potential of diurnal winds may be expected, since in moist environments such as the Amazon forest, surface warming promotes upward movements that increase the low-level moisture convergence and intensify convection. Moreover, the results from the nighttime period provide evidence on the importance of downdrafts on the propagation of extreme winds downward below the canopy.

4. Discussion

Coupling between the canopy and the atmosphere occurs when turbulence provides continuous mixing. At nighttime, however, the mixing can be inhibited by the presence of a stable layer. Therefore, two contrasting regimes are observed. In the weakly stable regime, the wind speed provides heat fluxes that are large enough to continuously transfer the energy lost by radiation back to the surface. In the very stable regime, heat fluxes are not transferred continuously to the surface, leading to strong temperature drops. This allows for the establishment of an enhanced thermal gradient, which further inhibits mixing. Thus, the coupling between the forest and the atmosphere is favored by the continuous turbulence observed in the weakly stable regime.

We evaluated the degree of coupling in two ways. First, a comparison of

σ_w on above (48 m) and sub-canopy heights following Thomas et al. (2013). Figure 11 shows the comparison between such variables but it is not easy to visualize the trends with only plotting the data points. Thus, we added a Locally Weighted Regression (LOWESS) to the graph (solid line). Here we focus on 4 forest understory heights (1.5 m, 7.0 m, 18.4 m and 31.6 m) and on datasets with and without downdrafts. During weak winds (i.e. without downdrafts), the turbulence strength at 1.5 m and 7.0 m was largely independent of that observed above canopy. After 18 m height, the $\sigma_w sub$ was linearly correlated with $\sigma_w top$ (Fig. 11c) indicating the occurrence of a coupled canopy condition. On the other hand, the extreme winds associated with downdrafts were propagated into the canopy at all heights, and the threshold of $\sigma_w top$ (i.e., when the correlation became linear) increased as flow above the canopy reached the ground.

Second, in order to quantify the coupling between the canopy and the atmosphere we calculated the temperature gradient (ΔT) between 51 m and 35 m height, in the dry and wet seasons. The dependence of ΔT on V (Fig. 12) shows the differences of coupling and subsequent mixing for the two regimes. A large thermal gradient occurs under the lowest wind speeds. This was observed when ΔT averaged 0.58 $^\circ C$ and 0.25 $^\circ C$ during the dry and wet seasons, respectively.

In the dry and wet seasons, ΔT peaked at V_L and reached 0.73 $^\circ C$ and 0.25 $^\circ C$, respectively. Similar ΔT maxima at the transition between regimes was observed by Acevedo et al. (2016) for the FLOSS II dataset. These authors argue that this pattern was associated with an enhanced heat-flux convergence at similar ranges of wind speed reported by Acevedo et al. (2021)

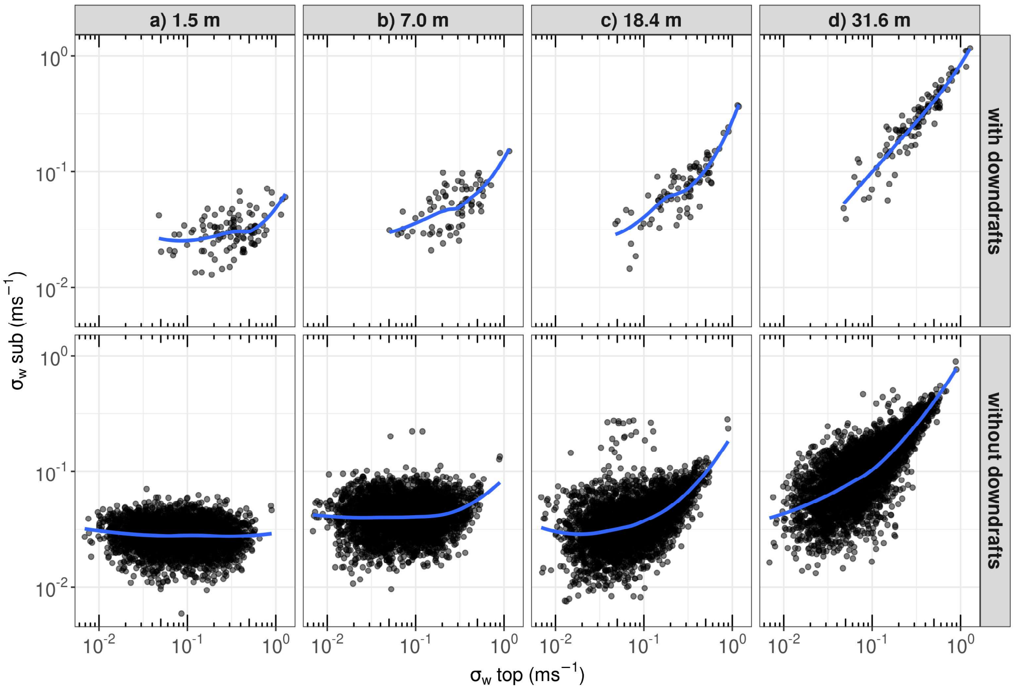

Figure 11: Standard deviation of wind vertical velocity (σ_w) between the forest understory (sub) and above-canopy (top at 48 m) heights. The dots correspond to periods of 5 min data. Dataset in which downdrafts occurred (Top panels). Dataset without the occurrence of downdrafts (Bottom panels). The columns a, b, c and d indicated the investigated sub-canopy heights.

for the CASES-99 dataset. Smaller gradients typical of mixed conditions occur when wind speeds are higher.

The relationship between turbulence and net radiation is a reliable criterium for distinguishing regimes. When the radiative loss is high, wind speeds tend to grow proportionally to allow compensative heat-fluxes (Acevedo et al., 2021). It is known that cloud cover plays an important role in R_N. Von Randow et al. (2004) showed that in the southern Amazon, reduced

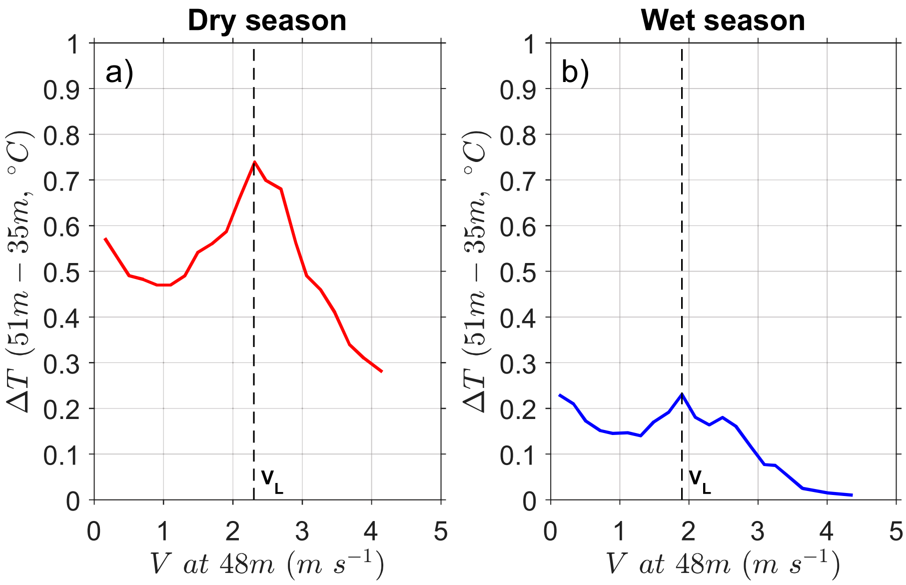

Figure 12: Differences of mean virtual temperature between 51 m and 35 m height as a function of the mean wind speed (V) at 48 m in the dry (a) and wet (b) season at the EEST, Manaus, Central Amazon. Dashed lines indicate the threshold wind speed (V_L) at which very stable changed to weakly stable regime.

cloud cover in the dry season results in increased radiative loss. The opposite occurs in the wet season. In this context, we have assessed the frequency distribution of R_N (30-min averages) for our studied period (from 8pm to 5am) and only for the nights in which downdrafts occurred (2h before and after respective events). In the dry season, the two lowest values of R_N (highest radiative loss) were observed between -40 and -60 $W\ m^{-2}$ (Fig. 13a). This variation indicates that there were relatively fewer clouds over the site. By contrast, R_N was more uniform during the wet season, with values ranging from -10 to -50 $W\ m^{-2}$ (Fig. 13b). Radiative loss was also higher in the 2-hour interval before and after downdrafts observed in the dry season (Fig.

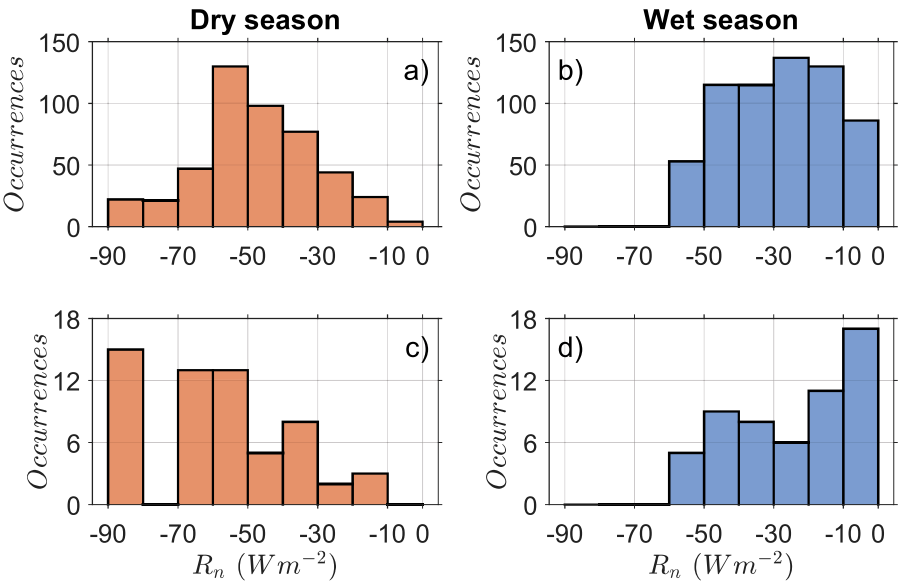

Figure 13: Distribution of the net radiation (R_n) for all studied days (top panels) and for those on which downdraft were identified (bottom panels) in the dry (red bars) and wet (blue bars) season during the nighttime.

13c,d).

This R_n pattern is related to the change in cloud cover and moisture loads at each season (Collow and Miller, 2016). Above the Amazon forest, single-cell clouds are frequent in the dry season. This contrasts mesoscale convective-systems (multiple cell) that are more frequent during the wet season (Gerken et al., 2016). Multiple cells and water vapor can trap some of the outgoing infrared radiation emitted by the Earth and radiate it back downward, which can reduce the radiative loss at the surface. This explains why the transition between regimes occurs at higher wind speed V_L in the dry season. During this period, the shallower cloud cover and the lower water vapor load of the atmospheric column allows for a larger loss of radiation than that observed in the wet period.

Both single and multiple cells are known to produce downdrafts (Gerken et al., 2016; Dias-Júnior et al., 2017b). Furthermore, we showed in this study that downdrafts are one of the main causes of transition from turbulence regimes above the Amazon forest (Fig. 9). We investigated the profile of four turbulent parameters during a night-time downdraft (July 24, 2014). H values, which were initially close to zero, turned strongly negative when the downdraft reached the tower at around 11 pm local time (Fig. 14a). Similarly, there was an increase in parameters associated with the intensity of turbulence, such as σ_w, TKE and friction velocity (u_*) (Figures 14b, c and d, respectively). Furthermore, this strong dissipation of air to strata/layers below the forest canopy are rarely observed in the absence of downdrafts. The air layer from the soil surface is largely decoupled from layers above the canopy (Thomas et al., 2013; Freundorfer et al., 2019; Cava et al., 2022). Santana et al. (2018) provided evidence that atmospheric eddies generated above the canopy can hardly penetrate the region below 0.5 h (h is the canopy top). This pattern was reported for different sites in the Amazon. However, observations (Bezerra et al., 2021) and numerical simulations (Serra-Neto et al., 2021) showed that under strong wind conditions, turbulence below the forest canopy was intensified and the scalar mixing more efficient.

The penetration of wind gusts inside the canopy increases the probability of tree damage and mortality. However, since the peak velocities may be underestimated when using single tower-measurements and we did not have data on risk of tree mortality, further studies are needed to describe the return frequency of such gusts and the relationship between speed and the

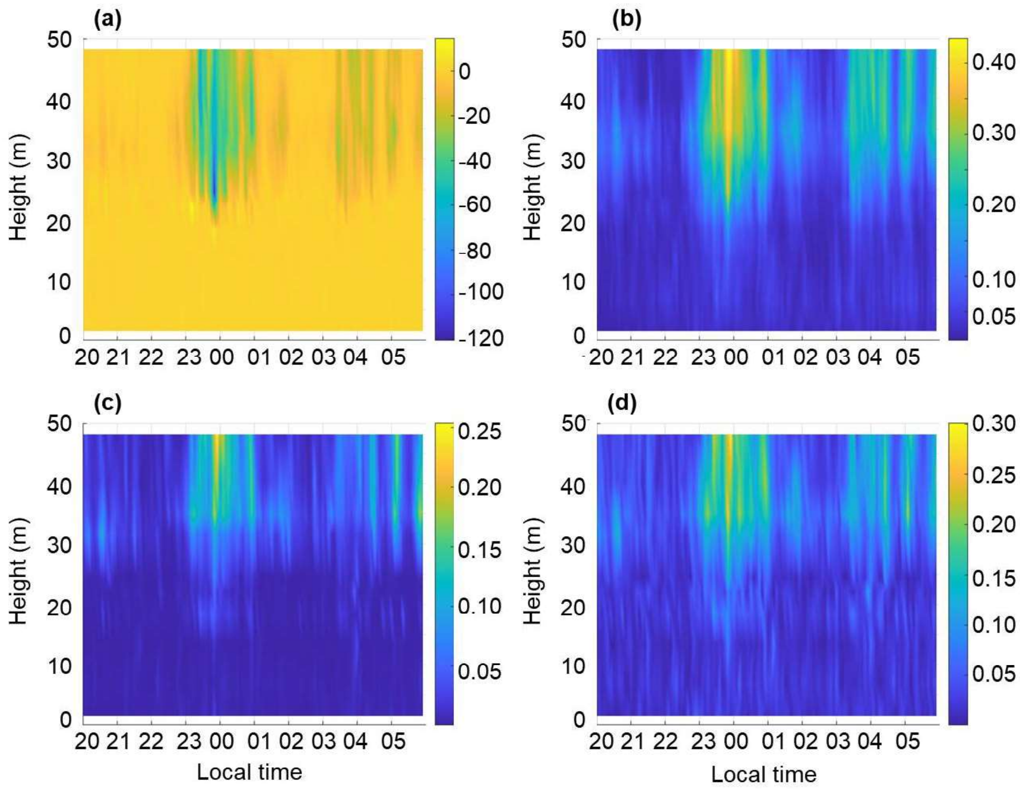

Figure 14: Vertical profile of: a) sensible heat flux (Wm^{-2}), b) standard deviation of vertical wind (ms^{-1}), c) Turbulent Kinetic Energy (m^2s^{-2}) and d) friction velocity (ms^{-1}) at the night of July 24, 2014.

disturbance severity.

Our study has limitations which shall be addressed in future research. First, the patterns we described for central Amazon may not occur in other regions with different vegetation structure. This highlights the need of studies based on extended datasets from other regions and for heights above 48 m. Second, when analyzing fast-response data from a single tower, the downdrafts may be not fully captured, and their magnitude and duration may be underestimated. Last, the link between wind speed, canopy structure and tree motion in these diverse forests is currently unknown. Nonetheless, our study stress the importance of datasets including a range of heights and seasons for detecting processes and mechanisms regulating turbulence and wind-tree interactions in dense tropical forests. A better understanding of these interactions is key for the parameterization of more robust and realistic in numerical models. In addition, our findings provided insights into the importance of wind gusts to the ecology and dynamics of Amazon forest.

5. Conclusions

This study provides three novel contributions. The first is the identification of different turbulence regimes and their patterns in terms of seasonality and proximity to the forest canopy in the nocturnal RSL. The second is the assessment of the effects of near surface wind gusts (propagated from downdrafts) on the organization of turbulence regimes. Finally, it provides evidences on the occurrance of extreme wind gusts associated with convective downdrafts, with potential do promote damage and mortality of canopy trees. These aspects highlight the strong interactions between atmospheric and biospheric processes and mechanisms regulating forest structure and dynamics.

Two turbulence regimes were identified: the very stable (weak turbulence) and weakly stable regime (strong turbulence). The wind speed threshold that mark the transition between the regimes increases nonlinearly with the distance from the ground under non-vegetated surfaces (Sun et al., 2012; Acevedo et al., 2021). Our study provides evidence that such pattern also occurs in closed canopy forests. In addition, new knowledge was obtained:

i) The average wind speed threshold for turbulence regime varies seasonally, and was relatively larger in the dry season at all heights as a consequence of a higher radiative loss from the surface during this period. Furthermore, the change of turbulence regime was influenced by the structure and roughness of the forest. This pattern was highlighted by relatively lower thresholds of wind speed compared to previous studies at mid-latitudes, and can be explained by the greater turbulent mixing above rough surfaces for a given mean wind speed.

ii) Near-surface wind gusts (convective downdrafts) occurred only during the weakly stable regime and were one of the main drivers of the observed turbulence regimes transition. Nevertheless, not all weakly stable regime were associated to such events.

iii) Full coupling state of wind flow among layers above and within the canopy occur during downdrafts. At nights without extreme winds, coupling along the canopy profile occurred only above 18 m height.

iv) The destructive potential of winds propagated during downdrafts was approximately four times higher than on nights without downdrafts in the wet season. By contrast, the wind speeds during daytime downdrafts were more intense in the dry season (not reported). These gusts would be sufficient to topple 73% of the previously investigated trees at our study site, which emphasize the importance of wind disturbances on controlling forest structure and diversity in central Amazon.

Acknowledgments

ACSM thanks the Conselho Nacional de Desenvolvimento Científico e Tecnológico (CNPq) for the Master grant awarded through the Programa de Pós-graduacão em Clima e Ambiente. This study is part of the Wind-Tree Interaction Project (INVENTA) and the Amazon Tall Tower Observatory (ATTO), funded by the German Federal Ministry of Education and Research (BMBF, contracts 01LB1001A and 01LK1602A), the Brazilian Ministry of Science, Technology and Innovation (MCTI/FINEP, contract 01.11.01248.00) and the Max Planck Society (MPG). ATTO is also supported by the Fundação de Amparo à Pesquisa do Estado do Amazonas (FAPEAM), Fundação de Amparo à Pesquisa do Estado de São Paulo (FAPESP), Universidade do Estado do Amazonas (UEA), Instituto Nacional de Pesquisas Amazônia (INPA), Programa de Grande Escala da Biosfera-Atmosfera na Amazônia (LBA) and the SDS/CEUC/RDS-Uatumã. We thank Marcelo Chameki and his team for the efforts in obtaining and making available the GoAmazon data.

References

Acevedo, O.C., Costa, F.D., Maroneze, R., Carvalho, Jr, A.D., Puhales, F.S., Oliveira, P.E.S., 2021. External controls on the transition between stable boundary-layer turbulence regimes. Quarterly Journal of the Royal Meteorological Society 147, 2335–2351. doi:10.1002/qj.4027.

Acevedo, O.C., Fitzjarrald, D.R., 2003. In the core of the night-effects of intermittent mixing on a horizontally heterogeneous surface. Boundary-layer meteorology 106, 1–33. doi:10.1023/A:1020824109575.

Acevedo, O.C., Mahrt, L., Puhales, F.S., Costa, F.D., Medeiros, L.E., Degrazia, G.A., 2016. Contrasting structures between the decoupled and coupled states of the stable boundary layer. Quarterly Journal of the Royal Meteorological Society 142, 693–702. doi:10.1002/qj.2693.

Alves, E.G., Jardine, K., Tota, J., Jardine, A., Yãnez Serrano, A.M., Karl, T., Tavares, J., Nelson, B., Gu, D., Stavrakou, T., Martin, S., Artaxo, P., Manzi, A., Guenther, A., 2016. Seasonality of isoprenoid emissions from a primary rainforest in central amazonia. Atmospheric Chemistry and Physics 16, 3903–3925. doi:10.5194/acp-16-3903-2016.

Araujo, R.F., Chambers, J.Q., Celes, C.H.S., Muller-Landau, H.C., Santos, A.P.F.d., Emmert, F., Ribeiro, G.H.P.M., Gimenez, B.O., Lima, A.J.N., Campos, M.A.A., Higuchi, N., 2020. Integrating high resolution drone imagery and forest inventory to distinguish canopy and understory trees and quantify their contributions to forest structure and dynamics. PLOS ONE 15, 1–16. doi:10.1371/journal.pone.0243079.

Araújo, A.C., Nobre, A.D., Kruijt, B., Elbers, J.A., Dallarosa, R., Stefani, P., von Randow, C., Manzi, A.O., Culf, A.D., Gash, J.H.C., Valentini, R., Kabat, P., 2002. Comparative measurements of carbon dioxide fluxes from two nearby towers in a central amazonian rainforest: The manaus lba site. Journal of Geophysical Research: Atmospheres 107, LBA 58–1–LBA 58–20. doi:10.1029/2001JD000676.

Betts, A.K., Gatti, L.V., Cordova, A.M., Silva Dias, M.A., Fuentes, J.D., 2002. Transport of ozone to the surface by convective downdrafts at night.

Journal of Geophysical Research: Atmospheres 107, LBA–13. doi:10.1029/2000JD000158.

Betts, A.K., et al., 2003. The diurnal cycle over land. Forests at the Land-Atmosphere Interface 79, 93.

Bezerra, V.L., Dias-Júnior, C.Q., Vale, R.S., Santana, R.A., Botía, S., Manzi, A.O., Cohen, J.C.P., Martins, H.S., Chamecki, M., Fuentes, J.D., 2021. Near-surface atmospheric turbulence in the presence of a squall line above a forested and deforested region in the central amazon. Atmosphere 12. doi:10.3390/atmos12040461.

Bonan, G.B., 2008. Forests and climate change: forcings, feedbacks, and the climate benefits of forests. science 320, 1444–1449. doi:10.1126/science.1155121.

Braga, P.I.S., 1979. Subdivisão fitogeográfica, tipos de vegetação, conservação e inventário florístico da floresta amazônica. Acta amazonica 9, 53–80.

Cava, D., Dias-Júnior, C.Q., Acevedo, O., Oliveira, P.E., Tsokankunku, A., Sörgel, M., Manzi, A.O., de Araújo, A.C., Brondani, D.V., Toro, I.M.C., et al., 2022. Vertical propagation of submeso and coherent structure in a tall and dense amazon forest in different stability conditions part i: Flow structure within and above the roughness sublayer. Agricultural and Forest Meteorology 322, 108983. doi:10.1016/j.agrformet.2022.108983.

Chambers, J.Q., Negron-Juarez, R.I., Marra, D.M., Di Vittorio, A., Tews, J., Roberts, D., Ribeiro, G.H.P.M., Trumbore, S.E., Higuchi, N., 2013. The steady-state mosaic of disturbance and succession across an old-growth central amazon forest landscape. Proceedings of the National Academy of Sciences 110, 3949–3954. doi:10.1073/pnas.1202894110.

Chambers, J.Q., Robertson, A.L., Carneiro, V.M., Lima, A.J., Smith, M.L., Plourde, L.C., Higuchi, N., 2009. Hyperspectral remote detection of niche partitioning among canopy trees driven by blowdown gap disturbances in the central amazon. Oecologia 160, 107–117. doi:10.1007/s00442-008-1274-9.

Chambers, J.Q., Tribuzy, E.S., Toledo, L.C., Crispim, B.F., Higuchi, N., Santos, J.d., Araújo, A.C., Kruijt, B., Nobre, A.D., Trumbore, S.E., 2004. Respiration from a tropical forest ecosystem: Partitioning of sources and low carbon use efficiency. Ecological Applications 14, 72–88. doi:10.1890/01-6012.

Chor, T.L., Dias, N.L., Araújo, A., Wolff, S., Zahn, E., Manzi, A., Trebs, I., Sá, M.O., Teixeira, P.R., Sörgel, M., 2017. Flux-variance and flux-gradient relationships in the roughness sublayer over the amazon forest. Agricultural and Forest Meteorology 239, 213–222. doi:10.1016/j.agrformet.2017.03.009.

Collow, A.B.M., Miller, M.A., 2016. The seasonal cycle of the radiation budget and cloud radiative effect in the amazon rain forest of brazil. Journal of Climate 29, 7703–7722. doi:10.1175/JCLI-D-16-0089.1.

Corrêa, P.B., Dias-Júnior, C.Q., Cava, D., Sörgel, M., Botía, S., Acevedo, O., Oliveira, P.E., Ocimar Manzi, A., Toledo Machado, L.A., dos Santos

Martins, H., Tsokankunku, A., de Araújo, A.C., Lavric, J.V., Walter, D., Mortarini, L., 2021. A case study of a gravity wave induced by amazon forest orography and low level jet generation. Agricultural and Forest Meteorology 307, 108457. doi:https://doi.org/10.1016/j.agrformet.2021.108457.

Costa, F.D., Acevedo, O.C., Medeiros, L.E., Maroneze, R., Puhales, F.S., Jr., A.D.C., Camponogara, L.F., dos Santos, D.M., Mortarini, L., 2020. Stable boundary layer regimes in single-column models. Journal of the Atmospheric Sciences 77, 2039 – 2054. doi:10.1175/JAS-D-19-0218.1.

Dias-Júnior, C.Q., Dias, N.L., Fuentes, J.D., Chamecki, M., 2017a. Convective storms and non-classical low-level jets during high ozone level episodes in the amazon region: An arm/goamazon case study. Atmospheric Environment 155, 199–209. doi:10.1016/j.atmosenv.2017.02.006.

Dias-Júnior, C.Q., Sá, L.D., Marques Filho, E.P., Santana, R.A., Mauder, M., Manzi, A.O., 2017b. Turbulence regimes in the stable boundary layer above and within the amazon forest. Agricultural and Forest Meteorology 233, 122–132. doi:10.1016/j.agrformet.2016.11.001.

D'Oliveira, F.A., Cohen, J.C., Spracklen, D.V., Medeiros, A.S., Cirino, G.G., Artaxo, P., Dias-Júnior, C.Q., 2022. Simulation of the effects of biomass burning in a mesoscale convective system in the central amazon. Atmospheric Research 278, 106345.

Espírito-Santo, F.D., Gloor, M., Keller, M., Malhi, Y., Saatchi, S., Nelson, B., Junior, R.C.O., Pereira, C., Lloyd, J., Frolking, S., et al., 2014. Size and frequency of natural forest disturbances and the amazon forest carbon balance. Nature communications 5, 1–6. doi:10.1038/ncomms4434.

Feng, Y., Negrón-Juárez, R.I., Romps, D.M., Chambers, J.Q., 2023. Amazon windthrow disturbances are likely to increase with storm frequency under global warming. Nature Communications 14, 101. doi:10.1038/s41467-022-35570-1.

Freundorfer, A., Rehberg, I., Law, B.E., Thomas, C., 2019. Forest wind regimes and their implications on cross-canopy coupling. Agricultural and Forest Meteorology 279, 107696. doi:https://doi.org/10.1016/j.agrformet.2019.107696.

Fuentes, J.D., Chamecki, M., dos Santos, R.M.N., Randow, C.V., Stoy, P.C., Katul, G., Fitzjarrald, D., Manzi, A., Gerken, T., Trowbridge, A., Freire, L.S., Ruiz-Plancarte, J., Maia, J.M.F., Tóta, J., Dias, N., Fisch, G., Schumacher, C., Acevedo, O., Mercer, J.R., Yañez-Serrano, A.M., 2016. Linking meteorology, turbulence, and air chemistry in the amazon rain forest. Bulletin of the American Meteorological Society 97, 2329 – 2342. doi:10.1175/BAMS-D-15-00152.1.

Fujita, T., 1985. The downburst: Microburst and macroburst. Satellite and Mesometeorology Research Project, Department of the Geophysical Sciences, University of Chicago 210, 122.

Garstang, M., Fitzjarrald, D.R., 1999. Observations of surface to atmosphere interactions in the tropics. Oxford University Press, USA. doi:10.1016/S0168-1923(03)00003-0.

Garstang, M., White, S., Shugart, H., Halverson, J., 1998. Convective cloud downdrafts as the cause of large blowdowns in the amazon rainforest. Meteorology and Atmospheric Physics 67, 199–212. doi:10.1007/BF01277510.

Gerken, T., Wei, D., Chase, R.J., Fuentes, J.D., Schumacher, C., Machado, L.A., Andreoli, R.V., Chamecki, M., Ferreira de Souza, R.A., Freire, L.S., Jardine, A.B., Manzi, A.O., Nascimento dos Santos, R.M., von Randow, C., dos Santos Costa, P., Stoy, P.C., Tóta, J., Trowbridge, A.M., 2016. Downward transport of ozone rich air and implications for atmospheric chemistry in the amazon rainforest. Atmospheric Environment 124, 64–76. doi:10.1016/j.atmosenv.2015.11.014.

Greco, S., Ulanski, S., Garstang, M., Houston, S., 1992. Low-level nocturnal wind maximum over the central amazon basin. Boundary-layer meteorology 58, 91–115. doi:10.1007/BF00120753.

Guerra, V.S., Acevedo, O.C., Medeiros, L.E., Oliveira, P.E., Santos, D.M., 2018. Small-scale horizontal variability of mean and turbulent quantities in the nocturnal boundary layer. Boundary-Layer Meteorology 169, 395–411. doi:10.1007/s10546-018-0381-3.

Knohl, A., Baldocchi, D.D., 2008. Effects of diffuse radiation on canopy gas exchange processes in a forest ecosystem. Journal of Geophysical Research: Biogeosciences 113. doi:10.1029/2007JG000663.

Machado, L., Laurent, H., Dessay, N., Miranda, I., 2004. Seasonal and diurnal variability of convection over the amazonia: A comparison of different vegetation types and large scale forcing. Theoretical and Applied Climatology 78, 61–77. doi:10.1007/s00704-004-0044-9.

Machado, L.A.T., Laurent, H., Lima, A.A., 2002. Diurnal march of the convection observed during trmm-wetamc/lba. Journal of Geophysical Research: Atmospheres 107, LBA 31–1–LBA 31–15. doi:10.1029/2001JD000338.

Mahrt, L., 1998. Nocturnal boundary-layer regimes. Boundary-layer meteorology 88, 255–278.

Mahrt, L., 2014. Stably stratified atmospheric boundary layers. Annual Review of Fluid Mechanics 46, 23–45. doi:10.1146/annurev-fluid-010313-141354.

Mahrt, L., Thomas, C., Richardson, S., Seaman, N., Stauffer, D., Zeeman, M., 2013. Non-stationary generation of weak turbulence for very stable and weak-wind conditions. Boundary-layer meteorology 147, 179–199. doi:10.1007/s10546-012-9782-x.

Malhi, Y., Meir, P., Brown, S., 2002. Forests, carbon and global climate. Philosophical Transactions of the Royal Society of London. Series A: Mathematical, Physical and Engineering Sciences 360, 1567–1591. doi:10.1098/rsta.2002.1020.

Marques Filho, A.d.O., Dallarosa, R.G., Pachêco, V.B., 2005. Radiação solar e distribuição vertical de área foliar em floresta-reserva biológica do cuieiras zf2, manaus. Acta Amazonica 35, 427–436. doi:10.1590/S0044-59672005000400007.

Marra, D.M., Chambers, J.Q., Higuchi, N., Trumbore, S.E., Ribeiro, G.H.P.M., dos Santos, J., Negrón-Juárez, R.I., Reu, B., Wirth, C., 2014. Large-scale wind disturbances promote tree diversity in a central amazon forest. PLOS ONE 9, 1–16. doi:10.1371/journal.pone.0103711.

Marra, D.M., Trumbore, S.E., Higuchi, N., Ribeiro, G.H.P.M., Negrón-Juárez, R.I., Holzwarth, F., Rifai, S.W., dos Santos, J., Lima, A.J.N., Kinupp, V.F., Chambers, J.Q., Wirth, C., 2018. Windthrows control biomass patterns and functional composition of amazon forests. Global Change Biology 24, 5867–5881. doi:10.1111/gcb.14457.

Melo, A.M., Dias-Junior, C.Q., Cohen, J.C., Sá, L.D., Cattanio, J.H., Kuhn, P.A., 2019. Ozone transport and thermodynamics during the passage of squall line in central amazon. Atmospheric Environment 206, 132–143. doi:https://doi.org/10.1016/j.atmosenv.2019.02.018.

Negrón-Juárez, R.I., Chambers, J.Q., Guimaraes, G., Zeng, H., Raupp, C.F.M., Marra, D.M., Ribeiro, G.H.P.M., Saatchi, S.S., Nelson, B.W., Higuchi, N., 2010. Widespread amazon forest tree mortality from a single cross-basin squall line event. Geophysical Research Letters 37. doi:10.1029/2010GL043733.

Negrón-Juárez, R.I., Holm, J.A., Marra, D.M., Rifai, S.W., Riley, W.J., Chambers, J.Q., Koven, C.D., Knox, R.G., McGroddy, M.E., Vittorio, A.V.D., Urquiza-Muñoz, J., Tello-Espinoza, R., Muñoz, W.A., Ribeiro, G.H.P.M., Higuchi, N., 2018. Vulnerability of amazon forests to storm-driven tree mortality 13, 054021. doi:10.1088/1748-9326/aabe9f.

Negrón-Juárez, R.I., Jenkins, H.S., Raupp, C.F.M., Riley, W.J., Kueppers, L.M., Magnabosco Marra, D., Ribeiro, G.H.P.M., Monteiro, M.T.F., Candido, L.A., Chambers, J.Q., Higuchi, N., 2017. Windthrow variability in central amazonia. Atmosphere 8. doi:10.3390/atmos8020028.

Nelson, B.W., 1994. Natural forest disturbance and change in the brazilian amazon. Remote Sensing Reviews 10, 105–125. doi:10.1080/02757259409532239.

Oliveira, A.N.d., Amaral, I.L.d., Ramos, M.B.P., Nobre, A.D., Couto, L.B., Sahdo, R.M., 2008. Composição e diversidade florístico-estrutural de um hectare de floresta densa de terra firme na amazônia central, amazonas, brasil. Acta amazônica 38, 627–641. doi:10.1590/S0044-59672008000400005.

Peterson, C.J., Ribeiro, G.H.P.d.M., Negrón-Juárez, R., Marra, D.M., Chambers, J.Q., Higuchi, N., Lima, A., Cannon, J.B., 2019. Critical wind speeds suggest wind could be an important disturbance agent in Amazonian forests. Forestry: An International Journal of Forest Research 92, 444–459. doi:10.1093/forestry/cpz025.

Ribeiro, G., Chambers, J., Peterson, C., Trumbore, S., Magnabosco Marra, D., Wirth, C., Cannon, J., Négron-Juárez, R., Lima, A., de Paula, E., Santos, J., Higuchi, N., 2016. Mechanical vulnerability and resistance to snapping and uprooting for central amazon tree species. Forest Ecology and Management 380, 1–10. doi:10.1016/j.foreco.2016.08.039.

Santana, R.A., Dias-Júnior, C.Q., da Silva, J.T., Fuentes, J.D., do Vale, R.S., Alves, E.G., dos Santos, R.M.N., Manzi, A.O., 2018. Air turbulence characteristics at multiple sites in and above the amazon rainforest canopy. Agricultural and Forest Meteorology 260, 41–54. doi:10.1016/j.agrformet.2018.05.027.

Santos, D.M., Acevedo, O.C., Chamecki, M., Fuentes, J.D., Gerken, T., Stoy, P.C., 2016. Temporal scales of the nocturnal flow within and above a forest canopy in amazonia. Boundary-Layer Meteorology 161, 73–98. doi:10.1007/s10546-016-0158-5.

dos Santos, L.T., Magnabosco Marra, D., Trumbore, S., de Camargo, P.B., Negrón-Juárez, R.I., Lima, A.J.N., Ribeiro, G.H.P.M., dos Santos, J., Higuchi, N., 2016. Windthrows increase soil carbon stocks in a central amazon forest. Biogeosciences 13, 1299–1308. doi:10.5194/bg-13-1299-2016.

Schwartz, N.B., Uriarte, M., DeFries, R., Bedka, K.M., Fernandes, K., Gutiérrez-Vélez, V., Pinedo-Vasquez, M.A., 2017. Fragmentation increases wind disturbance impacts on forest structure and carbon stocks in a western amazonian landscape. Ecological Applications 27, 1901–1915. doi:10.1002/eap.1576.

Serra-Neto, E.M., Martins, H.S., Dias-Júnior, C.Q., Santana, R.A., Brondani, D.V., Manzi, A.O., de Araújo, A.C., Teixeira, P.R., Sörgel, M., Mortarini, L., 2021. Simulation of the scalar transport above and within the amazon forest canopy. Atmosphere 12, 1631. doi:10.3390/atmos12121631.

Silvério, D.V., Brando, P.M., Bustamante, M.M.C., Putz, F.E., Marra, D.M., Levick, S.R., Trumbore, S.E., 2019. Fire, fragmentation, and windstorms:

A recipe for tropical forest degradation. Journal of Ecology 107, 656–667. doi:10.1111/1365-2745.13076.

Sun, J., Burns, S.P., Lenschow, D.H., Banta, R., Newsom, R., Coulter, R., Frasier, S., Ince, T., Nappo, C., Cuxart, J., et al., 2002. Intermittent turbulence associated with a density current passage in the stable boundary layer. Boundary-Layer Meteorology 105, 199–219. doi:10.1023/A:1019969131774.

Sun, J., Lenschow, D.H., LeMone, M.A., Mahrt, L., 2016. The role of large-coherent-eddy transport in the atmospheric surface layer based on cases-99 observations. Boundary-layer meteorology 160, 83–111. doi:10.1007/s10546-016-0134-0.

Sun, J., Mahrt, L., Banta, R.M., Pichugina, Y.L., 2012. Turbulence regimes and turbulence intermittency in the stable boundary layer during cases-99. Journal of Atmospheric Sciences 69, 338–351. doi:10.1175/JAS-D-11-082.1.

Sun, J., Takle, E.S., Acevedo, O.C., 2020. Understanding physical processes represented by the monin–obukhov bulk formula for momentum transfer. Boundary-Layer Meteorology 177, 69–95. doi:10.1007/s10546-020-00546-5.

Telles, E.d.C.C., de Camargo, P.B., Martinelli, L.A., Trumbore, S.E., da Costa, E.S., Santos, J., Higuchi, N., Oliveira Jr., R.C., 2003. Influence of soil texture on carbon dynamics and storage potential in tropical forest soils of amazonia. Global Biogeochemical Cycles 17. doi:10.1029/2002GB001953.

Thomas, C., Foken, T., 2007. Flux contribution of coherent structures and its implications for the exchange of energy and matter in a tall spruce canopy. Boundary-Layer Meteorology 123, 317–337. doi:10.1007/s10546-006-9144-7.

Thomas, C.K., Martin, J.G., Law, B.E., Davis, K., 2013. Toward biologically meaningful net carbon exchange estimates for tall, dense canopies: Multi-level eddy covariance observations and canopy coupling regimes in a mature douglas-fir forest in oregon. Agricultural and forest meteorology 173, 14–27. doi:10.1016/j.agrformet.2013.01.001.

Tóta, J., Fitzjarrald, D.R., da Silva Dias, M.A., 2012. Exchange of carbon between the atmosphere and the tropical amazon rainforest, in: Sudarshana, P., Nageswara-Rao, M., Soneji, J.R. (Eds.), Tropical Forests. IntechOpen, Rijeka. chapter 16. doi:10.5772/29716.

Urquiza Muñoz, J.D., Magnabosco Marra, D., Negrón-Juarez, R.I., Tello-Espinoza, R., Alegría-Muñoz, W., Pacheco-Gómez, T., Rifai, S.W., Chambers, J.Q., Jenkins, H.S., Brenning, A., Trumbore, S.E., 2021. Recovery of forest structure following large-scale windthrows in the northwestern amazon. Forests 12. doi:10.3390/f12060667.

Vickers, D., Göckede, M., Law, B., 2010. Uncertainty estimates for 1-h averaged turbulence fluxes of carbon dioxide, latent heat and sensible heat.

Tellus B: Chemical and Physical Meteorology 62, 87–99. doi:10.1111/j.1600-0889.2009.00449.x.

Vickers, D., Mahrt, L., 1997. Quality control and flux sampling problems for tower and aircraft data. Journal of Atmospheric and Oceanic Technology 14, 512 – 526. doi:10.1175/1520-0426(1997)014<0512:QCAFSP>2.0.CO;2.

Vignon, E., van de Wiel, B.J.H., van Hooijdonk, I.G.S., Genthon, C., van der Linden, S.J.A., van Hooft, J.A., Baas, P., Maurel, W., Traullé, O., Casasanta, G., 2017. Stable boundary-layer regimes at dome c, antarctica: observation and analysis. Quarterly Journal of the Royal Meteorological Society 143, 1241–1253. doi:10.1002/qj.2998.

Viswanadham, Y., Molion, L., Manzi, A., Sá, L., Filho, V.S., André, R., Nogueira, J., Santos, R.d., 1990. Micrometeorological measurements in amazon forest during gte/able 2a mission. Journal of Geophysical Research: Atmospheres 95, 13669–13682. doi:10.1029/JD095iD09p13669.

Von Randow, C., Manzi, A.O., Kruijt, B., De Oliveira, P., Zanchi, F.B., Silva, R.d., Hodnett, M.G., Gash, J.H., Elbers, J.A., Cardoso, F.L., et al., 2004. Comparative measurements and seasonal variations in energy and carbon exchange over forest and pasture in south west amazonia. Theoretical and Applied Climatology 78, 5–26. doi:10.1007/s00704-004-0041-z.

Wakimoto, R., 2015. Mesoscale meteorology— microbursts .

Zahn, E., Chor, T., Dias, N., 2016. A simple methodology for quality control of micrometeorological datasets. Am J Environ Eng 6, 135–142. doi:10.5923/s.ajee.201601.20.

Revision marked

Highlights

Turbulence regimes in the nocturnal roughness sublayer: interaction with deep convection and tree mortality in the Amazon

Anne C. S. Mendonça, Cléo Q. Dias-Júnior, Otávio C. Acevedo, Raoni A. Santana, Felipe D. Costa, Robinson I. Negrón-Juarez, Antônio O. Manzi, Susan E. Trumbore, Daniel. M. Marra

- The transition threshold of turbulence regimes is different between dry and wet seasons.
- Downdrafts are one of the main drives of the observed turbulence regimes transition.
- Extreme winds associated with downdrafts are propagated into the canopy at all heights.
- The destructive potential of winds was four times higher during downdrafts events ~~Vulnerability of Amazon forests to extreme winds.~~

Turbulence regimes in the nocturnal roughness sublayer: interaction with deep convection and tree mortality in the Amazon

Anne C. S. Mendonça[a], Cléo Q. Dias-Júnior[a,b,*], Otávio C. Acevedo[c], Raoni A. Santana[d], Felipe D. Costa[e], Robinson I. Negrón-Juarez[f], Antônio O. Manzi[g], Susan E. Trumbore[h], Daniel. M. Marra[h]

[a]*Amazonian National Research Institute (INPA-CLIAMB), Manaus, AM, Brazil*
[b]*Department of Physics, Federal Institute of Pará (IFPA), Belém, PA, Brazil*
[c]*Departamento de Física, Universidade Federal de Santa Maria, Santa Maria, RS, Brazil*
[d]*Institute of Engineering and Geosciences, Federal University of West Pará (UFOPA), Santarém, PA, Brazil*
[e]*Universidade Federal do Pampa, Alegrete, Brazil*
[f]*Lawrence Berkeley National Laboratory, Berkeley, CA, USA*
[g]*National Institute for Spatial Research (INPE), Cachoeira Paulista, SP, Brazil*
[h]*Biogeochemical Processes Department, Max Planck Institute for Biogeochemistry, Jena, Germany*

Abstract

We investigated the influence of seasonality and proximity to the forest canopy on nocturnal turbulence regimes in the roughness sublayer of a Central Amazon forest. Since convective systems of different scales are common in this region, we also analyzed the effect of extreme wind gusts (propagated from convective downdrafts) on the organization of the turbulence regimes, and their potential to cause the mortality of canopy trees. Our data include high-frequency winds, temperature and ozone concentration at different heights during the dry and wet seasons of 2014. In addi-

*Corresponding Author
Email address: cleo.quaresma@ifpa.edu.br (Cléo Q. Dias-Júnior)

tion, we used critical wind-speed data derived from a tree-winching experiment and a modeling study conducted in the same study site. Two different turbulence regimes were identified at three heights above the canopy: a weakly stable (WS) and a very stable regime (VS). The threshold wind speeds that mark the transition between turbulence regimes were larger during the dry season and increased as a function of the height above the canopy. The turbulent fluxes of sensible heat and momentum during the WS accounted for 88% of the entire nighttime flux. Downdrafts occurred only in the WS and favored a fully coupled state of wind flow along the canopy profile. The destructive potential of winds was four times higher than on nights without downdrafts. ~~We investigated the influence of seasonality and proximity to the forest canopy on nocturnal turbulence regimes in the roughness sublayer of a Central Amazon forest. For that, we applied different methods associated with the turbulent velocity scale, and analyzed the effect of convective downdrafts propagating extreme wind gusts above and within the forest canopy. Our data include monthly measurements of precipitation and high-frequency winds, temperature and ozone concentration at different heights during the dry and wet seasons of 2014. In addition, we used critical wind-speed data derived from a tree-winching experiment and a modeling study conducted in the same study site. Our results show that the threshold wind speeds that separate the very stable from weakly stable regimes were larger during the dry season, and increased as a function of the height above the canopy. Downdrafts occurred only in the weakly stable regime. The turbulent fluxes of sensible heat and momentum during the weakly stable regime accounted for 88% of the entire nighttime flux. The maximum~~

~~wind-speed observed during the weakly stable regime was approximately four times higher than the values registered on nights without downdrafts.~~

Keywords: Downdrafts, Extreme wind speed, Seasonality, Tropical forest, Turbulence regimes, Wind disturbance

1. Introduction

A growing number of observational and modeling studies show that the ~~Amazon~~ world's forests plays a key role in ~~regional and~~ global climate (Malhi et al., 2002; Bonan, 2008; Alves et al., 2016) and emphasize its importance to the water, radiation and surface-energy balance. All these are affected by exchanges of mass (water vapor, carbon dioxide, methane, ozone, and a variety of gases and particles), heat (sensible and latent) and momentum between the forest and the atmosphere (Von Randow et al., 2004; Thomas and Foken, 2007; Knohl and Baldocchi, 2008; Gerken et al., 2016, among others). This near-surface boundary layer that is dynamically influenced by vegetation is called the roughness sublayer (RSL). Particularly at night, the transport efficiency decreases above the forest, which inhibits its penetration into the canopy (Cava et al., 2022) and leads to a decoupling between the sub- and upper canopy flows (Thomas et al., 2013; Freundorfer et al., 2019; Cava et al., 2022) ~~Exchange processes of mass, heat and momentum are driven by turbulent vertical-motions, which are produced by air warming over the surface (i.e. thermal component) and the interactions between atmospheric flow and surface roughness (i.e. mechanical component).~~

~~Studies carried out in the Amazon region highlight the difficulties in correctly estimating turbulent fluxes, which can vary significantly for different~~

~~wind speeds (Dias-Júnior et al., 2017b; Dias-Júnior et al., 2018; Dias-Júnior et al., 2020; Dias-Jú~~ ~~It is also known that the turbulent flow within and above forest canopies is more complex compared to those found for flat and homogeneous surfaces (Raupach et al., 1996; Raupach et al., 2000; Raupach et al., 2007; Raupach et al., 2020; Raupac~~

Assessments of turbulent flow are challenging in the ~~NBL~~ nocturnal RSL, particularly during the occurrence of intense downdrafts ~~that cause significant changes in atmospheric dynamics and can interact with forest canopies causing widespread tree-mortality.~~ that typically originate within a convective system (e.g. squall lines, super-cell and single-cell thunderstorms). Intense downdrafts can develop when cooled air from evaporating precipitation sinks rapidly towards the ground. Such events transport relatively cooler and drier air from the troposphere to the lower levels leading to changes in the thermodynamic and kinematic properties of the near-surface air mass (Wakimoto, 2015). These downdrafts can extend to the surface in the form of sudden variations in the values of the wind, pressure, turbulent fluxes and a drop in equivalent potential temperature (Garstang and Fitzjarrald, 1999; Betts et al., 2002; Dias-Júnior et al., 2017a; Melo et al., 2019; D'Oliveira et al., 2022). Such phenomena can gain an interesting physical interpretation when ~~they are~~ the turbulence is classified into distinct turbulent nocturnal regimes. In mid-latitude regions for example, Mahrt (1998) categorized turbulence as "weakly stable" and "very stable" to differentiate the conditions of sustained and non-sustained turbulence, respectively. Sun et al. (2012) classified the turbulence regimes as either weak or strong, according to the relationship between Turbulent Kinetic Energy (TKE) and wind speeds. Subsequently, such terms have been widely used to refer to the regimes.

The weakly stable regime follows Monin-Obukhov similarity theory, which is used in most atmospheric models for expressing the surface layer. On the other hand, the same is not true in the very stable regime (Mahrt, 1998, 2014). In general, numerical schemes such as those used in numerical weather prediction and atmospheric models reproduce the occurrence of both ~~NBL~~ nocturnal turbulence regimes, but conditions that mark the transition between them depend on the parameterizations used to represent the eddy diffusivity (Costa et al., 2020). The transition between regimes is not universal, varying from one site to another. Such differences may be associated with local factors, for example by increased cloudiness (Acevedo and Fitzjarrald, 2003), surface roughness (Mahrt et al., 2013) and net nocturnal radiative loss (Sun et al., 2020; Acevedo et al., 2021).

Recent studies (Santos et al., 2016; Cava et al., 2022) have evidenced that the nature of the nocturnal-scalar exchange between the canopy and the overlying atmosphere is contrastingly dependent on the turbulence regime. While the weakly stable regime is dominated by turbulence, under very stable conditions a relatively larger fraction of the exchange is produced by non-turbulence motion with long time scales. This fact is particularly important for quantifying these fluxes since under very stable conditions the typical eddy-covariance methods might not properly capture the total exchange. Therefore, when assessing exchange patterns it is important to consider the following: Is the exchange seasonally dependent? If so, what seasonal processes affect the regimes? Is the nocturnal turbulence regime influenced by the frequency of convective downdrafts, which can affect the total canopy-atmosphere exchange of scalars? Therefore, experimental results obtained at different sites, such as in dense tropical forests, are essential to better understand the biosphere-atmosphere interaction and to improve existing knowledge on the nocturnal boundary layer. ~~provide a better understanding and better parameterization of the NBL.~~

From another perspective, in regions often covered by intense convective systems and convective cloud clusters, such as the Amazon region (Betts et al., 2002, 2003; Machado et al., 2002, 2004), the downdrafts may propagate strong downward wind gusts with high velocities (Fujita, 1985; Nelson, 1994; Garstang et al., 1998; Negrón-Juárez et al., 2010, 2017, 2018). When they reaches the surface, strong wind outflow with horizontal dimensions is propagated (Fujita, 1985; Garstang et al., 1998). These wind gusts can cause widespread tree damage and mortality through snapping and/or uprooting. These modes of tree mortality occur when the mechanical load caused by wind exceeds the resistance of the trunk or the root-soil anchorage (Nelson, 1994; Marra et al., 2014; Ribeiro et al., 2016).

~~It is also known that the Amazon region is often covered by convective cloud clusters and intense convective systems (Betts et al., 2002, 2003; Betts et al., 2002; Betts et~~ ~~Deep/strong convection may produce downdrafts, which propagate strong downward wind gusts with high velocities (Fujita, 1985; Fujita, 1994; Fujita, 1998; Fujita, 2010; F~~ ~~When a downdraft reaches the surface, strong wind outflow with horizontal dimensions is propagated (Fujita, 1985; Fujita, 1998). Such events transport relatively cooler and drier air to the lower levels leading to changes in the thermodynamic and kinematic properties of the near-surface air mass (Wakimoto, 2015). Apart from that, downdrafts can cause widespread tree damage and mortality through snapping and/or uprooting. These modes of tree mortality occur~~

~~when the mechanical load caused by wind exceeds the resistance of the trunk or the root-soil anchorage (Nelson, 1994; Nelson, 2014; Nelson, 2016).~~

The severity of damage/mortality caused by extreme wind events influences biomass balance and the functional composition of *terra-firme* forests in Central and Northwestern Amazon (Urquiza Muñoz et al., 2021; Negrón-Juárez et al., 2018; Marra et al., 2018, 2014). While some of the carbon contained in dead or damaged trees is decomposed and incorporated into the soil rather than directly emitted into the atmosphere (dos Santos et al., 2016), dead trees represent future CO_2 emissions (Chambers et al., 2004) and potentially methane (CH_4), which contributes to global warming. Using field data (Ribeiro et al., 2016) combined with static and dynamic biomechanical models, Peterson et al. (2019) estimated that wind speeds $> 10.75\ ms^{-1}$ are critical and can snap or uproot trees in *terra-firme* forests of Central Amazon.

Current knowledge about the effects of wind disturbances in the Amazon forest derives from studies that have quantified the spatial extent of these events using satellite imagery, in particular Landsat (Nelson, 1994; Negrón-Juárez et al., 2010; Chambers et al., 2013; Espírito-Santo et al., 2014), or from post-perturbation forest inventories to assess associated tree damage/mortality and their effects on forest structure and diversity in subsequent years to decades (Marra et al., 2014, 2018; Schwartz et al., 2017; Silvério et al., 2019; Urquiza Muñoz et al., 2021). The estimated time to recover 90% of pre-disturbance biomass is up to 40 years (Marra et al., 2018) in the Central Amazon and 30 years in the northwestern Amazon (Urquiza Muñoz et al., 2021).

The goal of our study was to identify the existence of different nocturnal turbulence regimes above a *terra-firme* forest in the Central Amazon and their possible association with seasonality and proximity to the forest canopy. Furthermore, to assess the effect of extreme winds associated with convective downdrafts on the organization of turbulence regimes in the nocturnal ~~boundary layer~~ RSL and the potential of observed winds to cause damage/mortality of canopy trees. We recognize that damaging winds and downdrafts in this region are also associated with convective storms and with fronts that can pass during the day, but that is beyond the scope of the current analysis. To our knowledge, this is the first assessment of the influence of extreme winds on turbulence regimes and of the potential of associated wind to promote tree damage/mortality. Apart from a better understanding of the ~~Amazon boundary layer structure and~~ processes of turbulent exchange between the biosphere and the atmosphere, especially in rainforests with dense canopies, our study provides insights into the vulnerability of Amazon forests to ongoing shifts on the intensity and frequency of convective storms resulting from climate change (Feng et al., 2023).

2. Material and methods

2.1. Study site and data acquisition

Our data were collected at the *Estação Experimental de Silvicultura Tropical* (EEST, also known as ZF2), Central Amazon, Brazil (Figure 1). The EEST is located about 60 km northwest of Manaus (2° $36'$ S, 60° $12'$ W, 130 m $a.s.l.$) (Araújo et al., 2002) and is predominantly covered by old-growth *terra-firme* forest with closed canopy (e.g. 593 ± 28 trees ha^{-1}), dense understory and high tree-species diversity (Braga, 1979; Marra et al., 2014). Trees are relatively tall and slender (Oliveira et al., 2008; Ribeiro et al., 2016). The proportion of trees reaching the canopy increased with diameter at breast height (DBH): from 21% for trees 10-20 cm DBH, and 57% for 20-30 cm DBH, up to 100% for trees above 70 cm DBH (Araujo et al., 2020).

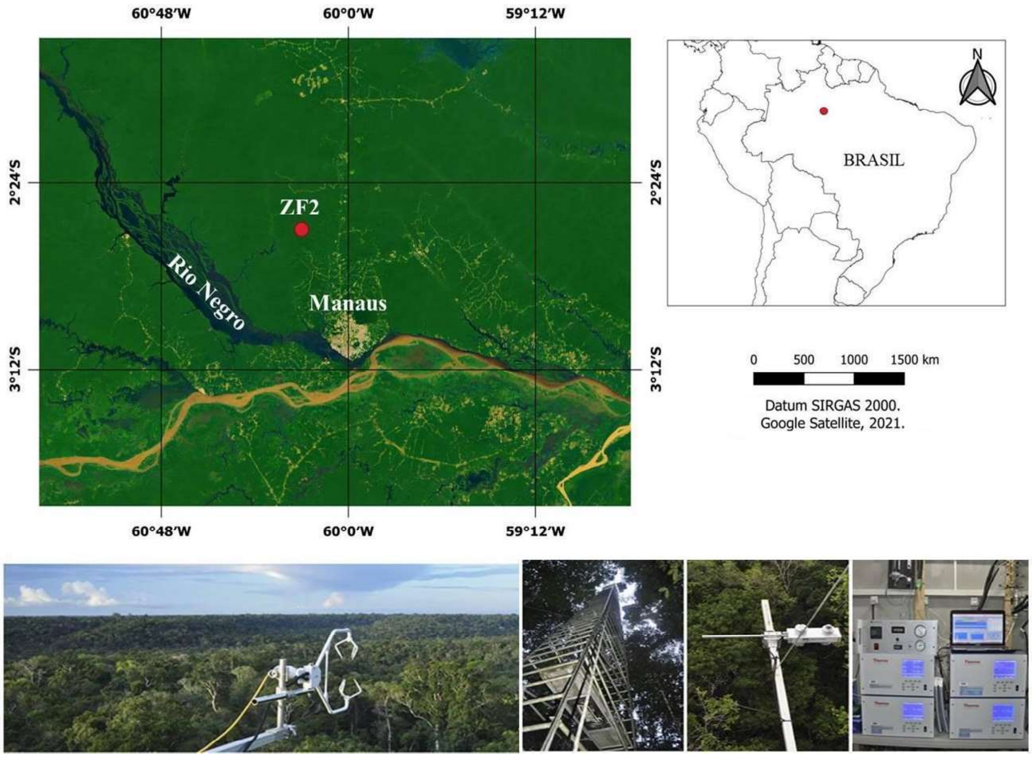

Figure 1: Study area at the *Estação Experimental de Silvicultura Tropical* (EEST) near Manaus, Brazil, and micrometeorological tower and sensors. (Top panel) Map of Brazil showing the study region. (Bottom left) A panoramic view of the forest and the employed 3D-sonic anemometer. (Bottom center left) Micrometeorological tower. (Bottom center right) Net radiometer. (Bottom right) Ozone analyzers.

The topography at the study area comprises a mosaic of plateaus, slopes and valleys with elevation differences of about 50 m. The vegetation cover on the plateau and slope areas is composed by forest with height varying between 30 to 40 m, maximum surface area density of 0.35 m^2m^{-3}. In valley areas, the vegetation is smaller with heights from 15 to 25 m, but with significant surface area density more than the 0.35 m^2m^{-3} (Tóta et al., 2012). The average values of leaf area index for the local vegetation was 6.1 m^2m^{-2} (Marques Filho et al., 2005).

Oxisols rich in kaolinite clay dominate plateaus and the upper portions of slopes. The soils on slope bottoms and valleys are sandy and mixed with organic matter (Spodosol) (Telles et al., 2003). The mean annual temperature is 27 °C and mean annual rainfall was about 2365 mm for the period between 1971 and 2000, with a distinct dry season between July and September (rainfall < 100 $mm\ month^{-1}$) (Negrón-Juárez et al., 2017).

Our data were collected using sensors installed on a micrometeorological tower of 54 m height. We used the sonic virtual temperature (T) and wind components (u, v and w) measured at 10 different heights (i.e. 1.5, 7.0, 13.5, 18.4, 22.1, 24.5, 31.6, 34.9, 40.4 and 48.2 m above ground) by 3D-sonic anemometers (model CSAT3, Campbell Scientific Inc., Logan, UT, USA) at a rate of 20 Hz. For analyzing the vertical temperature gradient, we used thermo-hygrometer data from sensors (HMP45AC, Vaisala) installed at 35.5 m and 51 m height. These data were available at a 30 min resolution. Net radiation (R_N) was measured with a net-radiometer (model CNR1, Kipp & Zonen, Delft, Netherlands) installed at 39 m height. We used data from April 2014 to January 2015 collected ~~on the scope~~ in the course of the Green Ocean Amazon Experiment (GoAmazon). For more details about instruments and respective measurements, see Fuentes et al. (2016).

Ozone concentration (O_3) was measured continuously at 40 m height at a frequency of 1 Hz using an ultraviolet light absorbed gas analyzer (model 49i, Thermo Fisher Scientific Inc., Waltham, MA). For more details on ozone measurements see Gerken et al. (2016). Convective cloud coverage over the study site was assessed with GOES-13 (Geostationary Operational Environmental Satellites) satellite imagery data available at the Brazilian National Institute for Space Research (INPE) database (http://satelite.cptec.inpe.br/acervo/, accessed on 30 May 2021).

Our data were analyzed for two time periods: (i) 55 days in the wet season (from April to May) and (ii) 36 days during the dry season (from July to September). To avoid transitional periods, we used data from 2000 to 0500 local standard time (LST). ~~for NBL~~. The dry and wet seasons were characterized based on the seasonality of precipitation using the Global precipitation Mission (GPM) level-3 product ($mm\ h^{-1}$). Estimates were carried out using data downloaded from the website of National Aeronautics and Space Administration (NASA) (https://giovanni.gsfc.nasa.gov, accessed on 28 october 2020) for the period between 1st April and 31st December 2014. Overall, we used a product of the Integrated Multi-satellitE Retrievals for GPM (IMERG) at a spatial resolution of 0.1° x 0.1° and at temporal resolution of 1 month (Final Run IMERGM v06). The IMERG algorithm combines information from the GPM satellite constellation and precipitation gauges. The system "final run" uses monthly gauge data to create research-level products.

Local estimates of critical wind-speed (CWS) were compiled from Peterson et al. (2019). According to these authors, the CWS is the wind speed necessary to generate a turning moment at the base of the trunk greater than or equal to the turning moment that results in tree failure. CWS were modeled based on critical turning moments measured locally in a winching experiment that included 60 trees from different species and varying sizes (Ribeiro et al., 2016). We considered CWS values estimated from a dynamic model (i.e. profile method) assuming that tree mortality associated with convective systems can create canopy gaps that contribute to increasing turbulence and wind propagation into the forest. In this model, tree spacing/density, leaf-area index and wind profiles are updated progressively after each tree failure (Peterson et al., 2019). The reported CWS ranged from 10.75 ms^{-1} to 34.5 ms^{-1}.

Before analyzing the micrometeorological, meteorological and profile data, we conducted the following quality control: (i) testing for record completeness and checking for the presence of error flags as proposed by Zahn et al. (2016) and (ii) detection of spikes and dropouts with eventual removal of corrupted/damaged data as suggested by Vickers and Mahrt (1997).

2.2. Turbulence regimes and flux estimates

In this study we examine the turbulence regimes at three heights. The first one was defined as near as possible to the top of the forest canopy (i.e. $\approx$ 35 m; Fuentes et al. (2016)), and the other two at the maximum heights where the sensors were installed on the tower (40 and 48 m, respectively). We focused only on the nighttime period (i.e., nocturnal boundary layer) because the diurnal relationship between wind speed and turbulence rarely deviates from linearity (not shown here), since typical daytime conditions at our study site are close to neutrality. ~~Since the physical processes associated with turbulence are completely different during daytime, here we focused only on the nighttime period (stable boundary layer). During daytime, the state of stable stratification is regularly overturned by the heating of the air layers that are in contact with the surface (i.e., boundary layer and surface are strongly coupled).~~

We used two methods for identifying the nocturnal turbulence regimes. The method proposed by Sun et al. (2012, 2016) considers the possibility of external agents (e.g. convective clouds) acting on the atmospheric boundary layer and disturbing its turbulent fields (Garstang et al., 1998; Garstang and Fitzjarrald, 1999; Betts et al., 2002; Dias-Júnior et al., 2017a). Sun's method accounts for the average relationship between the turbulent velocity scale (V_{TKE}) and the mean horizontal wind speed (V). Where $V_{TKE} = \sqrt{TKE} = [0.5({\sigma_u}^2+{\sigma_v}^2+{\sigma_w}^2)]^{1/2}$ and $V = \sqrt{u^2+v^2}$, in which u, v and w are zonal, meridional and vertical wind components, σ represents the standard deviation of each variable and TKE represents the Turbulent Kinetic Energy. Sun's method identifies the wind speed threshold value (V_L) from the slope change of a straight line around which the data are clustered. For this, we performed a segmented linear regression and selected the V_L with the best coefficient of determination (R^2). In this case, turbulence is compared at a given level with the wind speed at that level.

The second method, reported by Acevedo et al. (2016) is based on the sign inversion of the vertical gradient of V_{TKE} (ΔV_{TKE}). This procedure accounts for the relationship between V_{TKE} and V, but in contrast to Sun's method, turbulence is examined at all levels in terms of the wind speeds at a fixed reference level. When classified by the V at a reference level, the wind speed crossover threshold (V_T) lies where the average ΔV_{TKE} reverses sign for the entire tower layer. This change occurs because in very stable regime the V_{TKE} increase with height and the importance of low-frequency (sub mesoscale fluctuations) phenomena at higher levels contributes to this pattern. In weakly stable regime, on the other hand, the classical pattern of decreasing turbulence with height is dominant. Therefore, the parameters V_L and V_T are the wind speed values that determine the change from very stable (decoupled boundary layer) to weakly stable regime (the classical boundary layer coupled to the surface). Here, we assumed ΔV_{TKE} as the difference between 48 m and 35 m.

Fluxes were estimated by the Eddy Covariance method. We calculated the turbulent fluxes of sensible heat as $H = \rho c_p \overline{\theta' w'}$ and momentum as $\tau = \rho(\overline{u'w'}^2 + \overline{v'w'}^2)^{1/2}$, where ρ is the density of air (assumed to be 1.225 kgm^{-3}) and c_p is the specific heat of air at a constant pressure. The variables θ' and w', represent the fluctuations of virtual temperature (°C) and vertical wind speed (ms^{-1}), respectively. As suggested by Sun et al. (2002) and Vickers et al. (2010), we used mean values over 5 min intervals for all the different statistical moments of the turbulence.

To investigate statistical differences between the very stable and weakly stable regimes, we first used the Mann Whitney U-test considering the identified regimes as grouping variables. Therefore, six tests were performed, one at each height (48 m, 40 m and 35 m) and for the dry and wet seasons. In a second analysis, we applied a factorial analysis of variance (ANOVA) followed by Tukey tests to assess the effects of the interaction between the seasons, heights and turbulence regimes on observed patterns of atmospheric turbulence. Here we use V_{TKE} as dependent variable. For all tests we considered a significance level of 5% and used the software Matlab and Jamovi for data processing and analysis.

In this work V_{TKE} was only used in the analysis of the transition of turbulence regimes, but not as an indicator of the tree damage/mortality. To assess the potential of extreme wind gusts as a mechanism of tree damage/mortality, we compared the CWS data available for our study site and the maximum wind speed observed within our study period, as detailed in section 2.4.

2.3. Identification of convective cloud downdrafts

Previous studies have demonstrated that convective downdrafts transport air with high O_3 concentrations and lower T (cold pool) rapidly from the lower-middle troposphere to the surface (Betts et al., 2002; Gerken et al., 2016; Dias-Júnior et al., 2017a; Bezerra et al., 2021).

It is known that in environments with high moisture and strong convection such as in the Amazon, the equivalent potential temperature (θ_e) is also important under unstable atmospheric conditions. Since θ_e changes as a function of moisture (through mixing ratio) and temperature, the downward transport of cold and dry air leads to an important decrease of θ_e (Garstang and Fitzjarrald, 1999; Betts et al., 2002). However, moisture data were not available for our study site. Alternatively, we used virtual temperatures.

The identification of convective cloud downdrafts in our study was performed using a two-step procedure. We first analyzed the time series of horizontal wind speed, air temperature and surface concentration of O_3 to investigate atmospheric dynamics and the occurrence of gust fronts associated with convective clouds. For this analysis, we averaged data at 48 m (V and T) and 40 m (O_3) height for 5-minute intervals. The data series were mapped by an algorithm that identifies a subtle increase of O_3 concentrations of at least 3 parts per billion (ppb), and a simultaneous decrease of T values of 2 °C within a 1h time window of respective events (Gerken et al., 2016; Dias-Júnior et al., 2017a). During these events, the highest horizontal wind speed registered within one second interval and the five minutes average comprising such an interval were retained. False detections were manually identified and removed. In the next step, GOES-13 imagery were visually inspected for the presence of convective clouds over the study site. Here, we only considered images acquired on days for which abrupt changes in weather variables were detected as described in the previous step. We analyzed the effect of downdrafts associated with turbulence regimes by checking the relationship between V_{TKE} and V. Here, we assumed the minimum and maximum V values to determine the start and end time of respective wind gusts.

2.4. Extreme winds as a mechanism of tree mortality

To assess the potential of extreme wind gusts as a mechanism of tree damage/mortality, we compared the CWS data and the maximum wind speed (V_o) measured by our anemometers. The V_o is the maximum horizontal wind speeds (or extremes winds) measured at 5 min time-intervals at 48 m height. These data were analyzed for the different seasons (dry and wet).

Since downdrafts can last from few seconds to (rarely) minutes, we calculated V_o at two other time intervals: 1-minute and 30-seconds windows. To check if V_o differs with the size of time-intervals, we compared computed values (response variable) using ANOVA of repeated measures. Subsequently, we executed an ANOVA to verify potential variations of V_o as a function of seasonality.

3. Results

3.1. Turbulence regimes in the nocturnal boundary layer

We found a positive relationship between V_{TKE} and V for both dry and wet seasons, and a clear distinction between the two turbulence regimes (Figure 2). For events classified as weak turbulence (very stable regime), V_{TKE} increased less than V as indicated by a ~~relatively~~ smaller slope. As V reached a threshold value (V_L), turbulence changed from weak to strong (weakly stable regime) as indicated by a ~~relatively~~ larger increase of V_{TKE} as a function of V and larger slope. V_L increased nonlinearly with the distance from the forest canopy in both seasons. The observed values of V_L at 35 m and 48 m were near 0.7 and 2.3 ms^{-1} (dry) and 0.5 and 1.9 ms^{-1} (wet), respectively. These results are in agreement with previous studies that found that V_L increases nearly logarithmically with height (Sun et al., 2012; Acevedo et al., 2016).

Although the observed increase of V_L with height supports previous research on non-vegetated surfaces, the thresholds identified at 35 m in our study site were significantly smaller than those observed at a pasture area at the Federal University of Santa Maria (in south Brazil) (V_L of 3.0 ms^{-1} at 30 m height) (Acevedo et al., 2021) and at project FLOSS II (Fluxes over Snow Surfaces) conducted in Colorado (US) (V_L of 5.3 ms^{-1} at 30 m height)

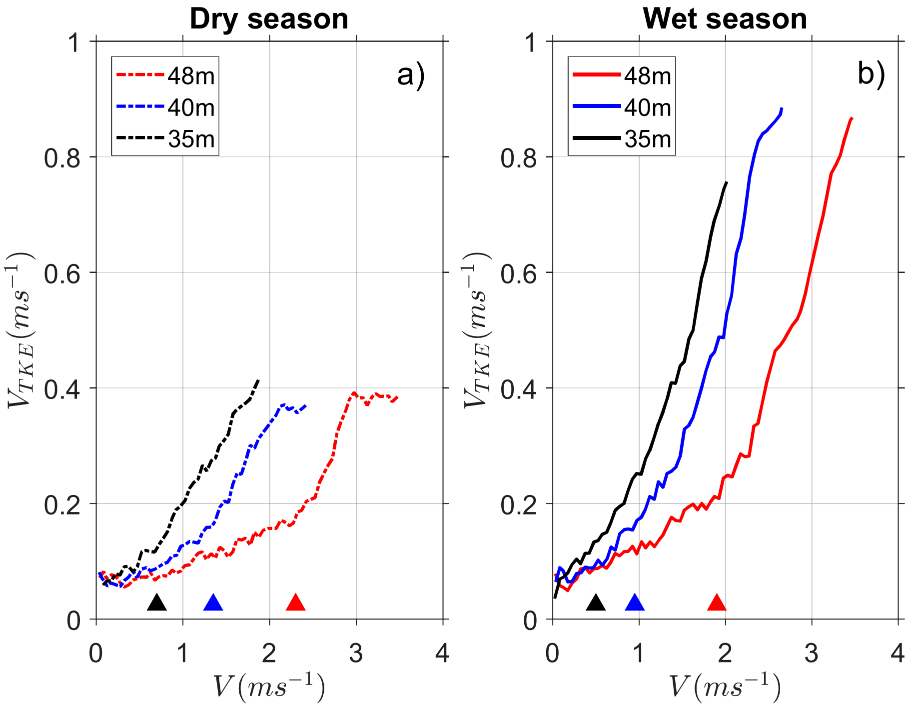

Figure 2: Relationship between turbulence velocity scale (V_{TKE}) and mean wind speed (V) at different heights in the (a) dry and (b) wet season during the nighttime at the EEST, Manaus, Central Amazon. Triangles indicate the threshold wind speed (V_L) at which the very stable changed to weakly stable regime.

(Acevedo et al., 2016). Such differences show that the structure and roughness of dense forests influence the change of the turbulence regime. ~~Similar to the analysis performed by Chor et al. (2017) for the Amazon Tall Tower Obsevatory (ATTO) site, we also used the zero-plane displacement height (d) equal to d = 0.9 h = 31.5 m (where h is the canopy height) at our study site. Therefore, a proper comparison must consider the observation level with respect to d.~~ For a proper comparison we considered the observation level with respect to the zero plane displacement height (d). We used d=31.5 m based on estimates provided by Viswanadham et al. (1990) and Chor et al. (2017) for central Amazon, in which d=0.88h and d=0.9h, respectively, where h is the canopy height (35 m at our study site). Doing that, the V_L values found at 35 m (z-d = 3.5 m) in both seasons are smaller than the value of 2.04 ms^{-1} found at 2 m in FLOSS II (Acevedo et al., 2016) and that of 1.5 ms^{-1} found at 1.5 m in the CASES-99 (experiment carried out in southeast Kansas, US) (Sun et al., 2012). Similarly, the V_L found for both seasons at the EEST at 48 m (z-d=16.5 m) are smaller than those at 15 m in FLOSS (5.04 ms^{-1}) and at 10 m in CASES-99 (4.5 ms^{-1}). The V_L found at 48 m at EEST site in the wet season is also smaller than the value reported by Acevedo et al. (2021) at 14 m in Santa Maria (2.2 ms^{-1}). Still, this value is close to that we found during the dry season at the EEST. In general, the V_L values between turbulence regimes was smaller at the EEST site than that reported in previous studies at similar heights, even when the zero-plane displacement height is taken into account. This relates to V_L being generally smaller above rough surfaces compared to smooth surfaces (Mahrt et al., 2013; Vignon et al., 2017; Guerra et al., 2018), a simple consequence of turbulent mixing being larger above a rough surface than above a smooth one at a same mean wind speed.

From the nighttime turbulence regimes identified at 48 m height, around 77% (dry) and 65% (wet) of them were associated with very stable regime. In contrast, weakly stable regime corresponded to 23% (dry) and 35% (wet) of the events. Furthermore, V_L was larger during the dry season than in the wet season at the three investigated heights (Figure 2 and Table 1). This result is in agreement with Acevedo et al. (2021), who showed that

V_L increases linearly with net radiative loss at the surface at three mid-latitude sites. According to these authors, the fully turbulence regime occurs when the mean wind speed is large enough to support heat fluxes capable of transferring back to the surface part of the energy lost radiatively. Therefore, such a minimum heat flux and corresponding minimum wind speeds must be larger when the net radiative loss is also larger. The relationship between V_L and R_N is further discussed in Section 4.

Table 1: Wind speed threshold (V_L) at studied heights for the dry and wet seasons at the EEST, Manaus, Central Amazon.

Season	V_L at 48m (ms^{-1})	V_L at 40m (ms^{-1})	V_L at 35m (ms^{-1})
Dry	2.3	1.35	0.7
Wet	1.9	0.95	0.5

We also identified the transition between regimes as a function of V at 35 m, for which the ΔV_{TKE} reverses sign for both dry and wet seasons (Acevedo et al., 2021). Figure 3 show that the V_{TKE} increased with height for weak winds in both seasons. When V at 35 m exceeds a sharp threshold, this pattern is reversed, so that V_{TKE} decreases with height under sufficiently strong winds. Such a threshold was approximately 0.65 ms^{-1} and 0.50 ms^{-1} for the dry and wet seasons, respectively. However, when the same analysis is performed in terms of V at 48 m (Figure 4), there was no gradient reversal and V_{TKE} decreased with height for all observed wind speeds.

These findings suggest that the relationship between V and V_{TKE} at the different heights is not trivial and may be associated with the occurrence of phenomena such as low-level jets and density currents (Greco et al., 1992;

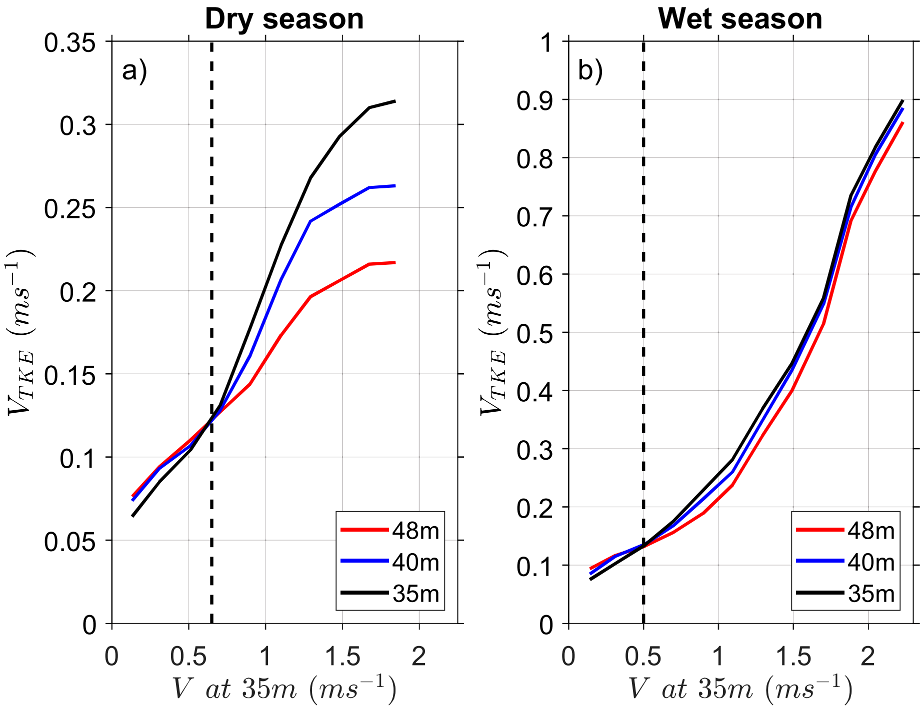

Figure 3: Turbulence velocity scale (V_{TKE}) as a function of the mean wind speed (V) at 35 m during the nighttime at the EEST, Manaus, Central Amazon. The solid lines are V_{TKE} at different heights in the (a) dry and (b) wet season. Black vertical dashed line indicates when V_{TKE} reverses its sign and exceeds the crossover threshold (V_T) at which the very stable changed to weakly stable regime

Dias-Júnior et al., 2017b; Corrêa et al., 2021). When the wind speeds are weak at higher levels, the wind profile is often distorted and maximum values can occur near the surface (Acevedo et al., 2016).

The V_T values identified by the vertical gradient method at 35 m height during the dry (0.65 ms^{-1}) and wet (0.50 ms^{-1}) seasons were similar to the V_L values obtained with Sun's method. This result corroborates the existence of nighttime turbulence regimes at the EEST during the two seasons. As the

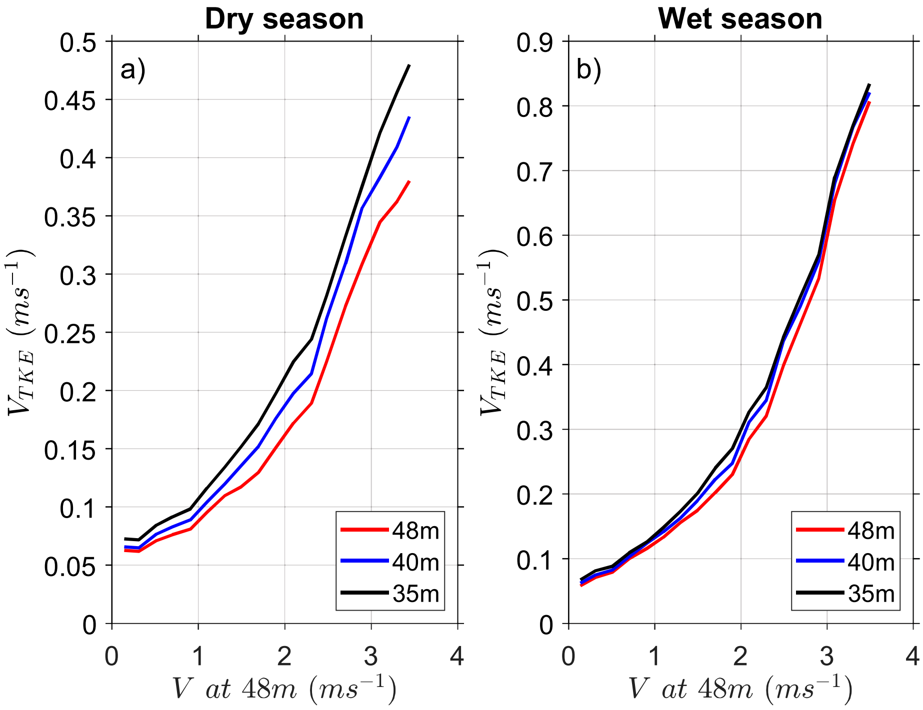

Figure 4: Turbulence velocity scale (V_{TKE}) as a function of the mean wind speed (V) at 48 m during the nighttime at the EEST, Manaus, Central Amazon. The solid lines are V_{TKE} at different heights in the (a) dry and (b) wet season

values of V_T and V_L were similar, hereafter we used the values of V_L as an indication for changes of turbulence regimes, since it was possible to identify it at all heights investigated here.

Our results evidenced the existence of different nocturnal turbulence regimes in the *terra-firme* Amazon forests. Moreover, they indicated that turbulence intensity decreased with the proximity to the canopy (Figure 5a). V_{TKE} during weakly stable regime was larger than in the very stable regime (Figure 5b). Overall, the wet season had larger values of V_{TKE} than the dry season (Figure 5c).

These larger values of V_{TKE} in the wet season are likely associated with a lower wind speed threshold between regimes in the wet season (Figure 2). Since the threshold is smaller, it is plausible considering that it is easier to overcome this threshold and establish "large" V_{TKE} in this case. Another reason that could result in larger values of V_{TKE} in the wet season would be simply because the wet season has higher wind speeds values than the dry season. Nonetheless, this was not the case, as can be seen in Figure 5d-f. Our result may be related to other factors, such as radiative loss, thermal gradient, among others.

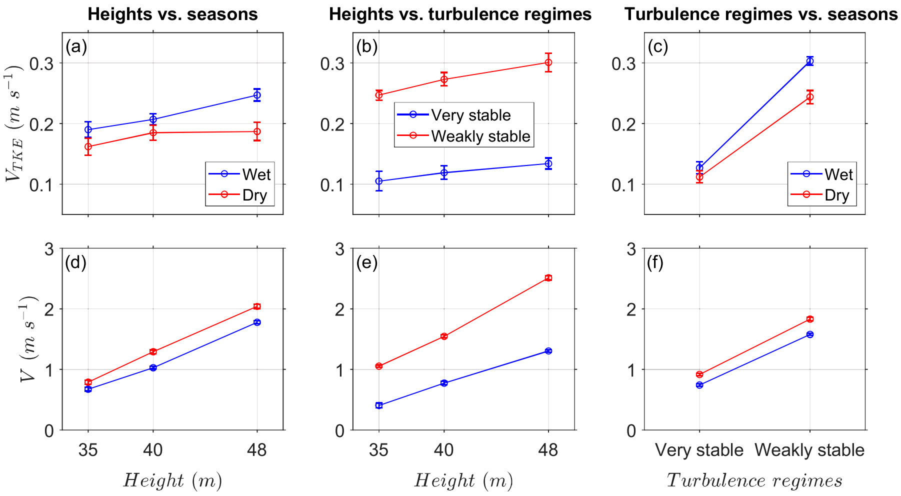

Figure 5: Turbulence velocity scale (V_{TKE}) and mean wind speed (V) as a function of (a,d) heights vs. seasons, (b,e) heights vs. turbulence regimes and (c,f) turbulence regimes vs. seasons during nighttime at the EEST, Manaus, Central Amazon. Legend: circles and vertical bars indicate mean values and the 95% confidence intervals, respectively

3.2. *Turbulent fluxes in the nocturnal boundary layer*

We investigated the differences between the turbulent fluxes during the occurrence of very stable and weakly stable regimes, and found an interesting relationship between V and the sensible heat (H), and momentum (τ) fluxes at 35 m height during both seasons. Bins of V each 0.2 ms^{-1} were used to calculate the average values and standard deviations of the fluxes. H values (Fig. 6a and Fig. 6b) changed in response to the turbulence shifting from the weak to the strong in both seasons (Table 2). On average, the H flux in the weakly stable regime corresponded to about 88% of the total H observed in both seasons. Our findings corroborate those of previous research conducted in Eastern Amazon (Dias-Júnior et al., 2017b). Importantly, H values were more intense during the dry season ($p = 0.001$). This result is possibly associated to larger net radiative loss due to reduced cloud cover and atmospheric column water vapor load (Collow and Miller, 2016), which leads to less longwave radiation reaching the canopy.

Table 2: Mean values ($\pm$ 95% confidence interval) of sensible heat flux (H) and momentum flux (τ) for the dry and wet seasons at the EEST, Central Amazon, Brazil.

Turbulence regimes	H Dry (Wm^{-2})	H Wet (Wm^{-2})	τ Dry (10^{-2}) (Nm^{-2})	τ Wet (10^{-2}) (Nm^{-2})
Very stable	-1.8 $\pm$2.5	-1.3 $\pm$2.0	-0.3 $\pm$ 0.4	-0.5 $\pm$ 0.6
Weakly stable	-13.4 $\pm$ 17	-9.8 $\pm$ 9.6	-2.3 $\pm$ 3.0	-4.1 $\pm$ 5.4

The τ fluxes showed a similar behavior to that of H, in which the flux in the weakly stable regime was larger than in the very stable regime ($p \leq$

0.001), and reached on average 89% of the total τ flux in each season (Fig. 6c and Fig. 6d). Such variations may be related to atmospheric stability conditions. The wet season is less stable (on average), that is, the strong turbulence events (i.e. weakly stable regime) occurs more frequently and, consequently, the momentum fluxes are greater. Overall, the weakly stable regime contributed more significantly to sensible heat and momentum fluxes than the very stable regime (Table 2), in both seasons.

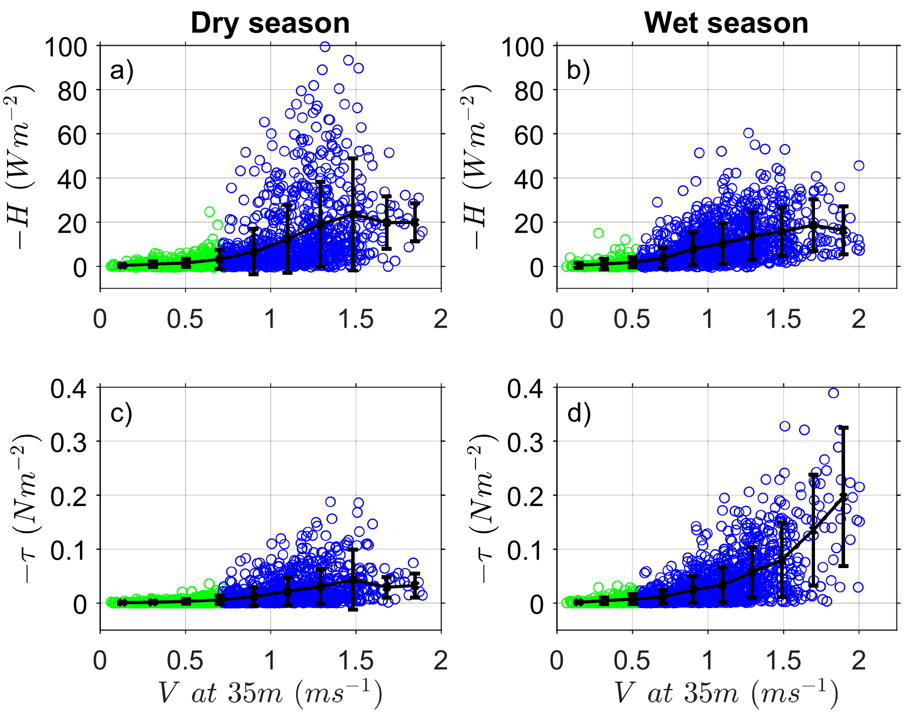

Figure 6: Mean and standard deviation of sensible heat flux (H) and momentum flux (τ) as a function of the wind speed (V) at 35 m during nighttime at the EEST, Manaus, Central Amazon. The left and right panels indicate the dry and wet season, respectively. Green and blue circles indicate the very stable and weakly stable regimes, respectively.

3.3. Relationship between deep convection and nocturnal turbulence regimes

During the night of 06 August 2014 and 12 April 2014, gust fronts from downdrafts reached the tower around 2110 LST (dry season) and 2325 LST (wet season), respectively (Figure 7). These events were evidenced from observations of (i) decreasing T (around 2 °C at both seasons) and (ii) simultaneous increasing O_3 of approximately 12 ppb (dry) and 15 ppb (wet). The pre-gust measurements of V ($\approx$ 2 ms^{-1}) were similar in both nights (Fig. 7c and Fig. 7g). However, V reached maximums of 7.5 (dry) and 15 ms^{-1} (wet) during the observed downdrafts. At this time, the standard deviation of wind vertical velocity (σ_w) increased substantially (Fig. 7d and Fig. 7h). As the surface cools and uncouples the boundary layer from the above troposphere, the near-surface O_3 values are low (3-5 ppb). This pattern allows for a clear recognition of night downdrafts transporting air with higher ozone and lower temperature to the surface. ~~Since the surface cools the NBL uncoupling. It from the layer above and thus reducing O_3 values (3-5 ppb), downdrafts are more easily recognized at night.~~ We observed this pattern on other nights and identified 16 downdrafts (eight different nights in each season) over the studied period. Overall, these events occurred between 2000 LST and 2300 LST. Finally, the GOES-13 imagery indicates the existence of cloudiness at the times of the events (Figure 8) and also on the other 16 nights that we studied here.

These results support previous studies, such as that by Betts et al. (2002) who found that nighttime convective downdrafts coupled the surface to the lower troposphere and transported down air with larger O_3 and lower equivalent potential temperature. Dias-Júnior et al. (2017a) also reported that

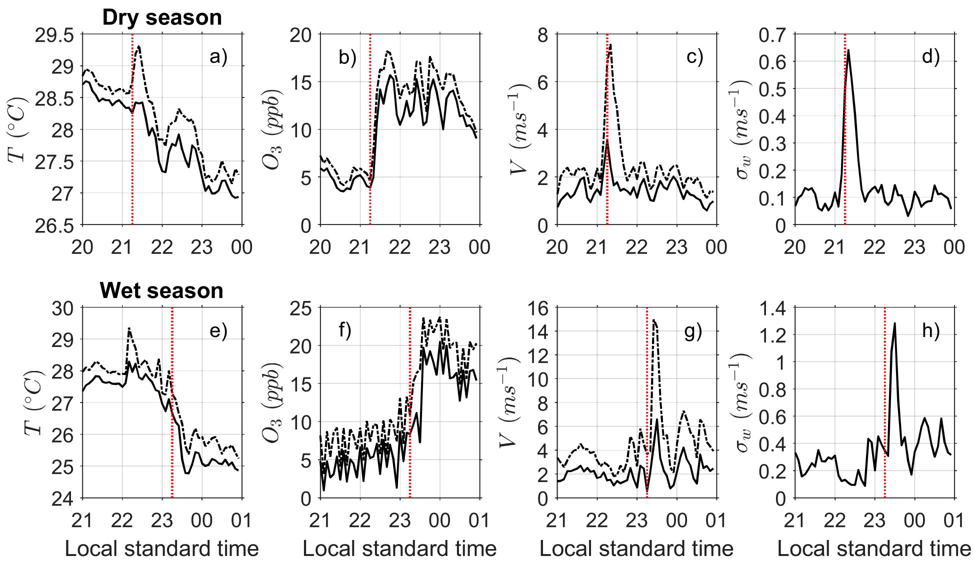

Figure 7: Times series of key variables used to identify downdrafts at the EEST, Central Amazon, Brazil. The upper and bottom panels show the downdrafts from 06 August 2014 and 12 April 2014, respectively. Legend: virtual temperature (T), ozone (O_3), horizontal wind speed (V) and standard deviation of wind vertical velocity (σ_w). Solid and dashed lines indicate the mean and maximum values, respectively. Vertical red-dotted lines indicate the starting time of downdrafts.

the downdrafts produce O_3 enhancement events and an increase in V values, in addition to the occurrence of air divergence during the horizontal propagation of density currents.

We observed that all downdrafts happened during or after the transition to the weakly stable regime (Figure 9). This pattern evidenced that downdrafts may influence the turbulence characteristics near the surface since they are associated with a weakly stable regime (strong turbulence). However, weakly stable regime was not represented completely by these events, which suggest that the strong turbulence may be associated with the occurrence

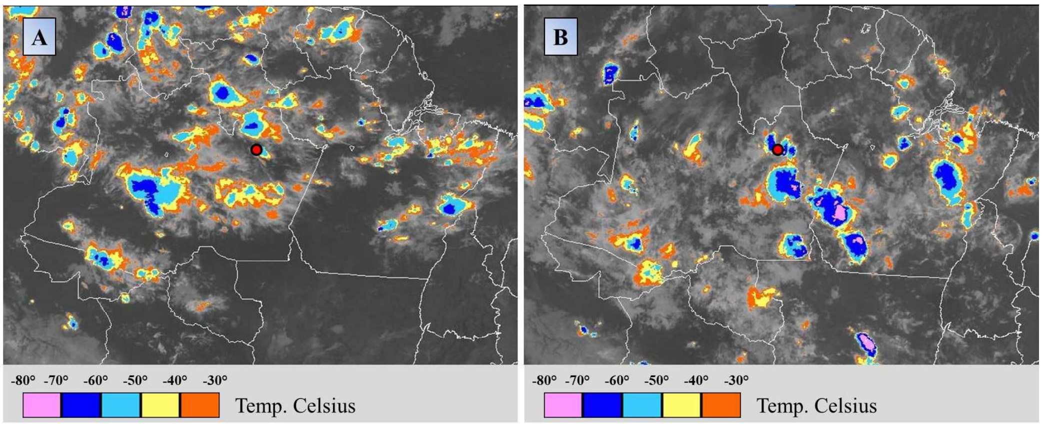

Figure 8: GOES 13 imagery for (a) 07 August 2014 at 0100 UTC and (b) 13 April 2014 at 0300 UTC when downdrafts reached the micrometeorology tower at the EEST (red dot), Central Amazon, Brazil.

of other phenomena. Similar results were previously reported for Central Amazon by Bezerra et al. (2021), who observed that downdrafts generated by a squall line occurred only during the strong turbulence regime.

3.4. Extreme winds as a mechanism of tree mortality

During the weakly stable regime associated with nocturnal downdraft events, the speeds and thus destructive potential of winds varied between seasons. The greatest wind speeds were identified during the wet season (V_o= 14.96 ms^{-1}). This value was approximately four times higher than on nights without downdrafts, and exceed the CWS of three out of the studied trees by Peterson et al. (2019). In contrast, maximum wind speeds in the nocturnal period of the dry season (V_o= 7.57 ms^{-1}) did not exceed the CWS of the studied trees.

Here we did not assess the direct effect of high wind-speeds on trees,

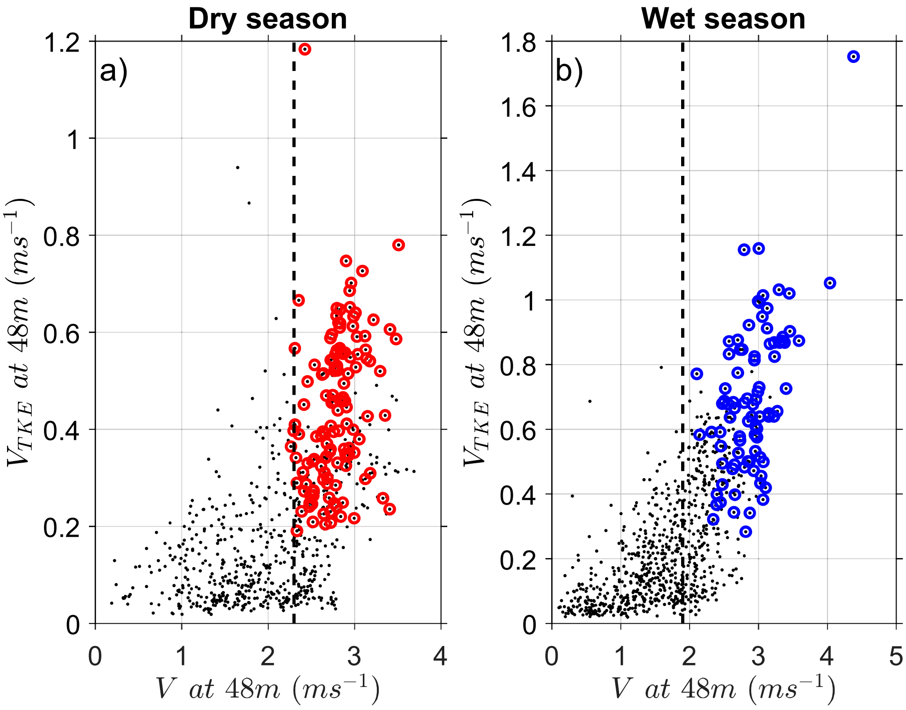

Figure 9: Turbulence velocity scale (V_{TKE}) as a function of the mean wind speed (V) measured at 48 m in the (a) dry and (b) wet season during nighttime at the EEST, Manaus, Central Amazon. The dots correspond to mean values calculated over 5-min periods. Thick circles indicate the range of occurrence of the downdrafts. Vertical black-dashed lines mark the threshold wind speed (V_L) at which the very stable changed to weakly stable regime.

but rather evaluated the destructive potential of these based on observational data acquired at the same study site. Importantly, the occurrence of excessive wind speeds does not necessarily result in trees damage and mortality. Further studies are needed to understand the link between wind speeds, canopy structure and tree motion in these diverse forests. Still, the strong dissipation of air to layers below the forest canopy (presented in Section 4) are rarely observed in the absence of downdrafts. Therefore, the wind gusts described in our study not only reached extreme speeds but also penetrated the forest canopy, and had the potential to cause damage and mortality of trees of different sizes, both directly and indirectly.

The mean V_o values varied significantly between the analyzed time-intervals ($p \leq 0.001$, Fig. 10a). As expected, the values were higher for the 30 seconds interval (5.97 ± 2.85 ms^{-1}, mean $\pm$ 95% confidence interval). For the 1 min and 5 min intervals, V_o was 5.35 ± 2.68 ms^{-1} and 3.63 ± 2.45 ms^{-1}, respectively. Results from subsequent ANOVA showed that the interaction between seasons and time intervals was significant ($p \leq 0.001$, Fig. 10b). Post-hoc Tukey tests showed that observed variations in V_o were not significantly different between seasons at both 1 min ($p = 0.057$) and 5 min ($p = 1.000$) intervals. Nonetheless, V_o varied as a function of seasonality for our shorter time interval (i.e. 30 seconds). These result shows that for extreme wind gusts that may last a few seconds such as those causing tree damage and mortality in the Amazon, our 30 second interval is likely too large and may have underestimated maximum V_o values.

Although daytime patterns were not a focal aspect in our study, wind speed reached the highest values (up to 22 ms^{-1}) during this period, in the dry season. In contrast to the relatively low destructive potential of nocturnal winds, this value could topple 73% of trees previously investigated in our study site (Ribeiro et al., 2016; Peterson et al., 2019). These observations reinforce the importance of extreme wind as a major natural mechanism of tree damage and mortality in these forests (Nelson, 1994; Chambers et al., 2009, 2013; Negrón-Juárez et al., 2017, 2018; Marra et al., 2018).

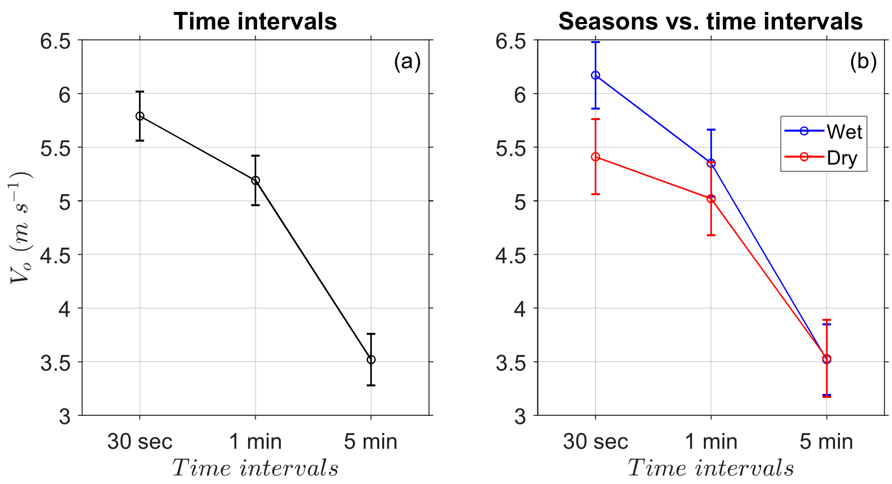

Figure 10: Observed wind speed (V_o) as a function of the (a) three time intervals and (b) seasons vs. time intervals at the EEST, Manaus, Central Amazon. Legend: circles and vertical bars indicate mean values and the 95% confidence intervals, respectively.

In fact, a higher destructive potential of diurnal winds may be expected, since in moist environments such as the Amazon forest, surface warming promotes upward movements that increase the low-level moisture convergence and intensify convection. Moreover, the results from the nighttime period provide evidence on the importance of downdrafts on the propagation of extreme winds downward below the canopy.

4. Discussion

Coupling between the canopy and the atmosphere occurs when turbulence provides continuous mixing. At nighttime, however, the mixing can be inhibited by the presence of a stable layer. Therefore, two contrasting regimes are observed. In the weakly stable regime, the wind speed provides heat fluxes that are large enough to continuously transfer the energy lost by radiation back to the surface. In the very stable regime, heat fluxes are not transferred continuously to the surface, leading to strong temperature drops. This allows for the establishment of an enhanced thermal gradient, which further inhibits mixing. Thus, the coupling between the forest and the atmosphere is favored by the continuous turbulence observed in the weakly stable regime.

We evaluated the degree of coupling in two ways. First, a comparison of σ_w on above (48 m) and sub-canopy heights following Thomas et al. (2013). Figure 11 shows the comparison between such variables but it is not easy to visualize the trends with only plotting the data points. Thus, we added a Locally Weighted Regression (LOWESS) to the graph (solid line). Here we focus on 4 forest understory heights (1.5 m, 7.0 m, 18.4 m and 31.6 m) and on datasets with and without downdrafts. During weak winds (i.e. without downdrafts), the turbulence strength at 1.5 m and 7.0 m was largely independent of that observed above canopy. After 18 m height, the $\sigma_w sub$ was linearly correlated with $\sigma_w top$ (Fig. 11c) indicating the occurrence of a coupled canopy condition. On the other hand, the extreme winds associated with downdrafts were propagated into the canopy at all heights, and the threshold of $\sigma_w top$ (i.e., when the correlation became linear) increased as flow above the canopy reached the ground.

Second, in order to quantify the coupling between the canopy and the atmosphere we calculated the temperature gradient (ΔT) between 51 m and 35 m height, in the dry and wet seasons. The dependence of ΔT on V (Fig. 12) shows the differences of coupling and subsequent mixing for the two regimes. A large thermal gradient occurs under the lowest wind speeds.

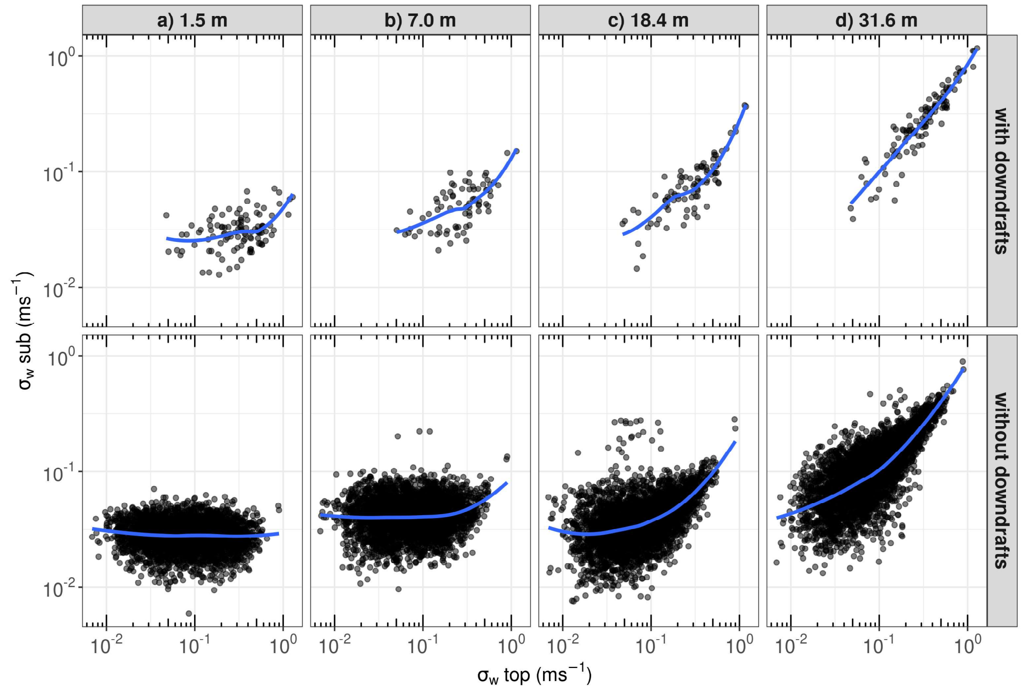

Figure 11: Standard deviation of wind vertical velocity (σ_w) between the forest understory (sub) and above-canopy (top at 48 m) heights. The dots correspond to periods of 5 min data. Dataset in which downdrafts occurred (Top panels). Dataset without the occurrence of downdrafts (Bottom panels). The columns a, b, c and d indicated the investigated sub-canopy heights.

This was observed when ΔT averaged 0.58 $°C$ and 0.25 $°C$ during the dry and wet seasons, respectively.

In the dry and wet seasons, ΔT peaked at V_L and reached 0.73 $°C$ and 0.25 $°C$, respectively. Similar ΔT maxima at the transition between regimes was observed by Acevedo et al. (2016) for the FLOSS II dataset. These authors argue that this pattern was associated with an enhanced heat-flux convergence at similar ranges of wind speed reported by Acevedo et al. (2021)

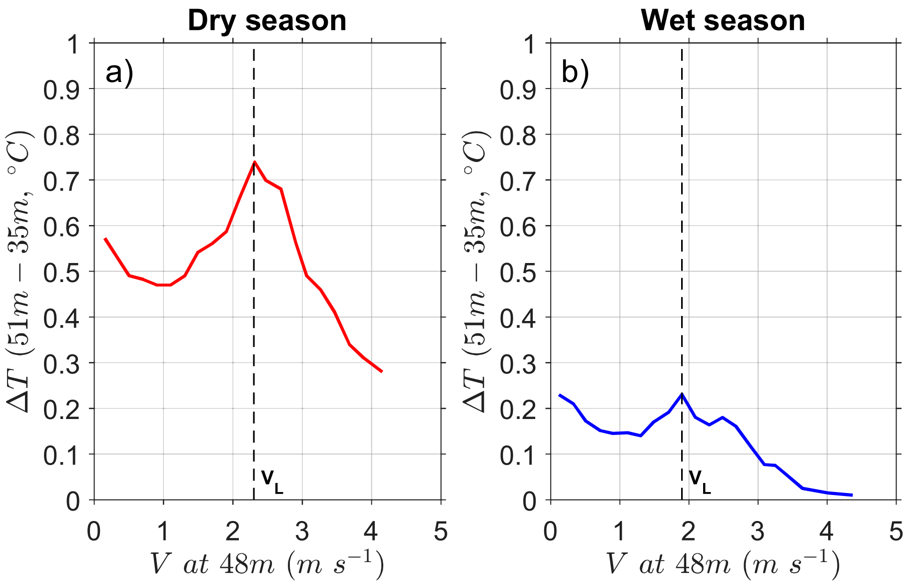

Figure 12: Differences of mean virtual temperature between 51 m and 35 m height as a function of the mean wind speed (V) at 48 m in the dry (a) and wet (b) season at the EEST, Manaus, Central Amazon. Dashed lines indicate the threshold wind speed (V_L) at which very stable changed to weakly stable regime.

for the CASES-99 dataset. Smaller gradients typical of mixed conditions occur when wind speeds are higher.

The relationship between turbulence and net radiation is a reliable criterium for distinguishing regimes. When the radiative loss is high, wind speeds tend to grow proportionally to allow compensative heat-fluxes (Acevedo et al., 2021). It is known that cloud cover plays an important role in R_N. Von Randow et al. (2004) showed that in the southern Amazon, reduced cloud cover in the dry season results in increased radiative loss. The opposite occurs in the wet season. In this context, we have assessed the frequency distribution of R_N (30-min averages) for our studied period (from 8pm to

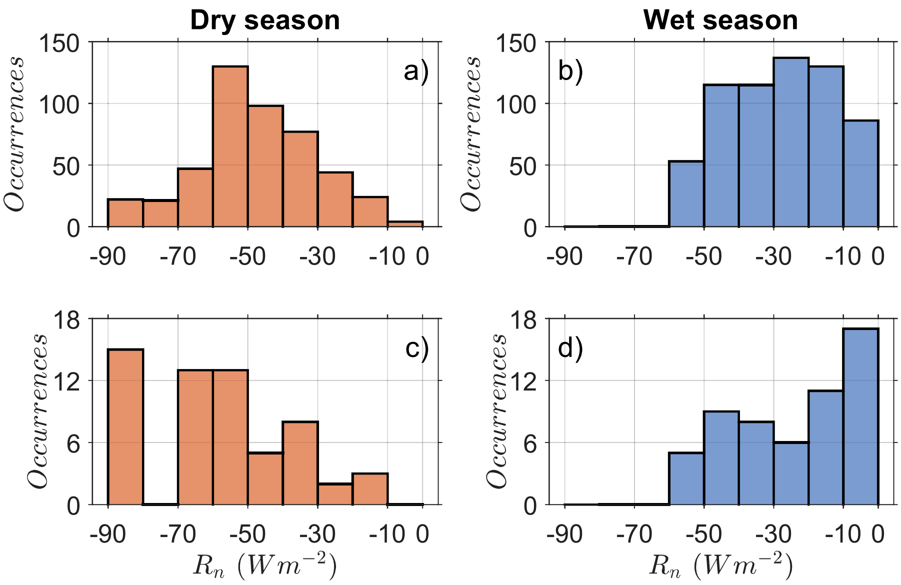

Figure 13: Distribution of the net radiation (R_n) for all studied days (top panels) and for those on which downdraft were identified (bottom panels) in the dry (red bars) and wet (blue bars) season during the nighttime.

5am) and only for the nights in which downdrafts occurred (2h before and after respective events). In the dry season, the two lowest values of R_N (highest radiative loss) were observed between -40 and -60 $W\ m^{-2}$ (Fig. 13a). This variation indicates that there were relatively fewer clouds over the site. By contrast, R_N was more uniform during the wet season, with values ranging from -10 to -50 $W\ m^{-2}$ (Fig. 13b). Radiative loss was also higher in the 2-hour interval before and after downdrafts observed in the dry season (Fig. 13c,d).

This R_n pattern is related to the change in cloud cover and moisture loads at each season (Collow and Miller, 2016). Above the Amazon forest, single-cell clouds are frequent in the dry season. This contrasts mesoscale convective-systems (multiple cell) that are more frequent during the wet season (Gerken et al., 2016). Multiple cells and water vapor can trap some of the outgoing infrared radiation emitted by the Earth and radiate it back downward, which can reduce the radiative loss at the surface. This explains why the transition between regimes occurs at higher wind speed V_L in the dry season. During this period, the shallower cloud cover and the lower water vapor load of the atmospheric column allows for a larger loss of radiation than that observed in the wet period.

Both single and multiple cells are known to produce downdrafts (Gerken et al., 2016; Dias-Júnior et al., 2017b). Furthermore, we showed in this study that downdrafts are one of the main causes of transition from turbulence regimes above the Amazon forest (Fig. 9). We investigated the profile of four turbulent parameters during a night-time downdraft (July 24, 2014). H values, which were initially close to zero, turned strongly negative when the downdraft reached the tower at around 11 pm local time (Fig. 14a). Similarly, there was an increase in parameters associated with the intensity of turbulence, such as σ_w, TKE and friction velocity (u_*) (Figures 14b, c and d, respectively). Furthermore, this strong dissipation of air to strata/layers below the forest canopy are rarely observed in the absence of downdrafts. ~~It is know that~~ The air layer from the soil surface ~~to 0.5 h (h is the canopy top)~~ is largely decoupled from layers above the canopy (Thomas et al., 2013; Freundorfer et al., 2019; Cava et al., 2022). Santana et al. (2018) provided evidence that atmospheric eddies generated above the canopy can hardly penetrate the region below 0.5 h (h is the canopy top). This pattern was reported for different sites in the Amazon. However, observations (Bezerra et al., 2021) and numerical simulations (Serra-Neto et al., 2021) showed that under strong wind conditions, turbulence below the forest canopy was intensified and the scalar mixing more efficient.

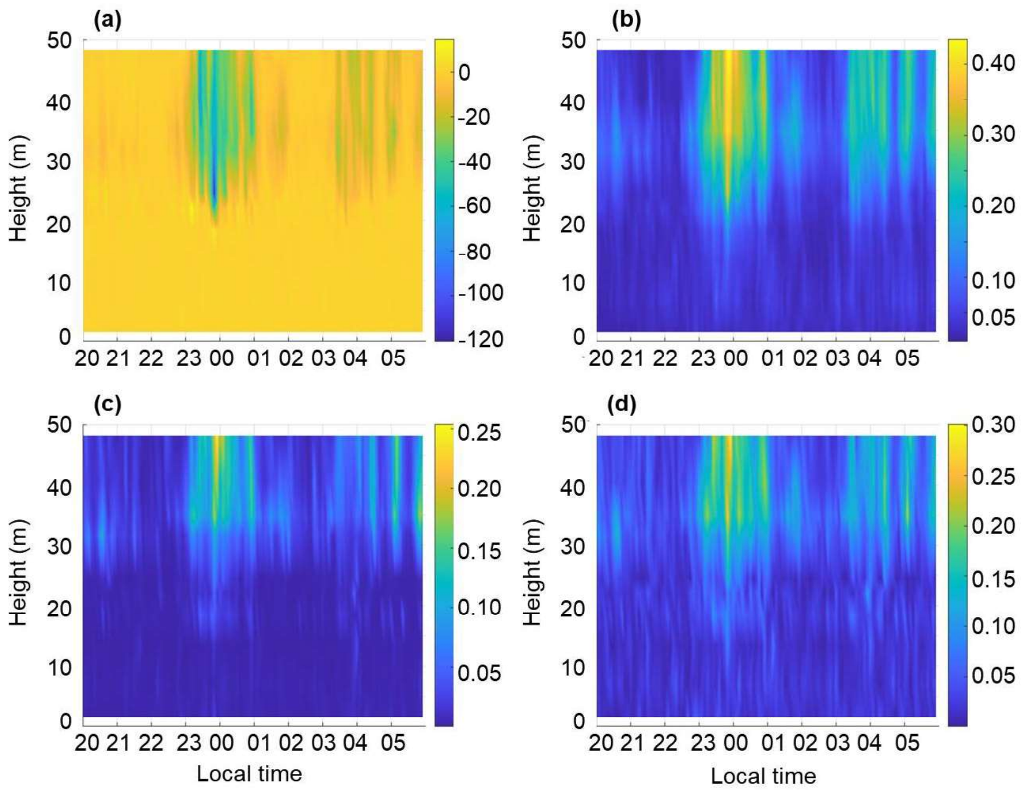

Figure 14: Vertical profile of: a) sensible heat flux (Wm^{-2}), b) standard deviation of vertical wind (ms^{-1}), c) Turbulent Kinetic Energy (m^2s^{-2}) and d) friction velocity (ms^{-1}) at the night of July 24, 2014.

The penetration of wind gusts inside the canopy increases the probability of tree damage and mortality. However, since the peak velocities may be underestimated when using single tower-measurements and we did not have data on risk of tree mortality, further studies are needed to describe the return frequency of such gusts and the relationship between speed and the disturbance severity.

Our study has limitations which shall be addressed in future research. First, the patterns we described for central Amazon may not occur in other regions with different vegetation structure. This highlights the need of studies based on extended datasets from other regions and for heights above 48 m. Second, when analyzing fast-response data from a single tower, the downdrafts may be not fully captured, and their magnitude and duration may be underestimated. Last, the link between wind speed, canopy structure and tree motion in these diverse forests is currently unknown. Nonetheless, our study stress the importance of datasets including a range of heights and seasons for detecting processes and mechanisms regulating turbulence and wind-tree interactions in dense tropical forests. A better understanding of these interactions is key for the parameterization of more robust and realistic in numerical models. In addition, our findings provided insights into the importance of wind gusts to the ecology and dynamics of Amazon forest.

5. Conclusions

This study provides three novel contributions. The first is the identification of different turbulence regimes and their patterns in terms of seasonality and proximity to the forest canopy in the ~~NBL~~ nocturnal RSL. The second is the assessment of the effects of near surface wind gusts (propagated from downdrafts) on the organization of turbulence regimes. Finally, it provides evidences on the occurrance of extreme wind gusts associated with convective downdrafts, with potential do promote damage and mortality of canopy trees. These aspects highlight the strong interactions between atmospheric and biospheric processes and mechanisms regulating forest structure and dynamics.

Two turbulence regimes were identified: the very stable (weak turbulence) and weakly stable regime (strong turbulence). The wind speed threshold that mark the transition between the regimes increases nonlinearly with the distance from the ground under non-vegetated surfaces (Sun et al., 2012; Acevedo et al., 2021). Our study provides evidence that such pattern also occurs in closed canopy forests ~~of central Amazon~~ . In addition, new knowledge was obtained:

i) The average wind speed threshold for turbulence regime varies seasonally, and was relatively larger in the dry season at all heights as a consequence of a higher radiative loss from the surface during this period. Furthermore, the change of turbulence regime was influenced by the structure and roughness of the forest. This pattern was highlighted by relatively lower thresholds of wind speed compared to previous studies at mid-latitudes, and can be explained by the greater turbulent mixing above rough surfaces for a given mean wind speed.

ii) Near-surface wind gusts (convective downdrafts) occurred only during the weakly stable regime and were one of the main drivers of the observed turbulence regimes transition. Nevertheless, not all weakly stable regime were associated to such events.

iii) Full coupling state of wind flow among layers above and within the canopy occur during downdrafts. At nights without extreme winds, coupling along the canopy profile occurred only above 18 m height.

iv) The destructive potential of winds propagated during downdrafts was approximately four times higher than on nights without downdrafts in the wet season. By contrast, the wind speeds during daytime downdrafts were more intense in the dry season (not reported). These gusts would be sufficient to topple 73% of the previously investigated trees at our study site, which emphasize the importance of wind disturbances on controlling forest structure and diversity in central Amazon.

Acknowledgments

ACSM thanks the Conselho Nacional de Desenvolvimento Científico e Tecnológico (CNPq) for the Master grant awarded through the Programa de Pós-graduacão em Clima e Ambiente. This study is part of the Wind-Tree Interaction Project (INVENTA) and the Amazon Tall Tower Observatory (ATTO), funded by the German Federal Ministry of Education and Research (BMBF, contracts 01LB1001A and 01LK1602A), the Brazilian Ministry of Science, Technology and Innovation (MCTI/FINEP, contract 01.11.01248.00) and the Max Planck Society (MPG). ATTO is also supported by the Fundação de Amparo à Pesquisa do Estado do Amazonas (FAPEAM), Fundação de Amparo à Pesquisa do Estado de São Paulo (FAPESP), Universidade do Estado do Amazonas (UEA), Instituto Nacional de Pesquisas Amazônia (INPA), Programa de Grande Escala da Biosfera-Atmosfera na Amazônia (LBA) and the SDS/CEUC/RDS-Uatumã. We thank Marcelo Chameki and his team for the efforts in obtaining and making available the GoAmazon data.

References

Acevedo, O.C., Costa, F.D., Maroneze, R., Carvalho, Jr, A.D., Puhales, F.S., Oliveira, P.E.S., 2021. External controls on the transition between stable boundary-layer turbulence regimes. Quarterly Journal of the Royal Meteorological Society 147, 2335–2351. doi:10.1002/qj.4027.

Acevedo, O.C., Fitzjarrald, D.R., 2003. In the core of the night-effects of intermittent mixing on a horizontally heterogeneous surface. Boundary-layer meteorology 106, 1–33. doi:10.1023/A:1020824109575.

Acevedo, O.C., Mahrt, L., Puhales, F.S., Costa, F.D., Medeiros, L.E., Degrazia, G.A., 2016. Contrasting structures between the decoupled and coupled states of the stable boundary layer. Quarterly Journal of the Royal Meteorological Society 142, 693–702. doi:10.1002/qj.2693.

Alves, E.G., Jardine, K., Tota, J., Jardine, A., Yãnez Serrano, A.M., Karl, T., Tavares, J., Nelson, B., Gu, D., Stavrakou, T., Martin, S., Artaxo, P., Manzi, A., Guenther, A., 2016. Seasonality of isoprenoid emissions from a primary rainforest in central amazonia. Atmospheric Chemistry and Physics 16, 3903–3925. doi:10.5194/acp-16-3903-2016.

Araujo, R.F., Chambers, J.Q., Celes, C.H.S., Muller-Landau, H.C., Santos, A.P.F.d., Emmert, F., Ribeiro, G.H.P.M., Gimenez, B.O., Lima, A.J.N., Campos, M.A.A., Higuchi, N., 2020. Integrating high resolution drone imagery and forest inventory to distinguish canopy and understory trees and quantify their contributions to forest structure and dynamics. PLOS ONE 15, 1–16. doi:10.1371/journal.pone.0243079.

Araújo, A.C., Nobre, A.D., Kruijt, B., Elbers, J.A., Dallarosa, R., Stefani, P., von Randow, C., Manzi, A.O., Culf, A.D., Gash, J.H.C., Valentini, R., Kabat, P., 2002. Comparative measurements of carbon dioxide fluxes from two nearby towers in a central amazonian rainforest: The manaus lba site. Journal of Geophysical Research: Atmospheres 107, LBA 58–1–LBA 58–20. doi:10.1029/2001JD000676.

Betts, A.K., Gatti, L.V., Cordova, A.M., Silva Dias, M.A., Fuentes, J.D., 2002. Transport of ozone to the surface by convective downdrafts at night. Journal of Geophysical Research: Atmospheres 107, LBA–13. doi:10.1029/2000JD000158.

Betts, A.K., et al., 2003. The diurnal cycle over land. Forests at the Land-Atmosphere Interface 79, 93.

Bezerra, V.L., Dias-Júnior, C.Q., Vale, R.S., Santana, R.A., Botía, S., Manzi, A.O., Cohen, J.C.P., Martins, H.S., Chamecki, M., Fuentes, J.D., 2021. Near-surface atmospheric turbulence in the presence of a squall line above a forested and deforested region in the central amazon. Atmosphere 12. doi:10.3390/atmos12040461.

Bonan, G.B., 2008. Forests and climate change: forcings, feedbacks, and the climate benefits of forests. science 320, 1444–1449. doi:10.1126/science.1155121.

Braga, P.I.S., 1979. Subdivisão fitogeográfica, tipos de vegetação, conservação e inventário florístico da floresta amazônica. Acta amazonica 9, 53–80.

Brunet, Y., 2020. Turbulent flow in plant canopies: Historical perspective and overview. Boundary-Layer Meteorology 177, 315–364.

Cava, D., Dias-Júnior, C.Q., Acevedo, O., Oliveira, P.E., Tsokankunku, A., Sörgel, M., Manzi, A.O., de Araújo, A.C., Brondani, D.V., Toro, I.M.C., et al., 2022. Vertical propagation of submeso and coherent structure in a tall and dense amazon forest in different stability conditions part i: Flow structure within and above the roughness sublayer. Agricultural and Forest Meteorology 322, 108983. doi:10.1016/j.agrformet.2022.108983.

Chambers, J.Q., Negron-Juarez, R.I., Marra, D.M., Di Vittorio, A., Tews, J., Roberts, D., Ribeiro, G.H.P.M., Trumbore, S.E., Higuchi, N., 2013. The steady-state mosaic of disturbance and succession across an old-growth central amazon forest landscape. Proceedings of the National Academy of Sciences 110, 3949–3954. doi:10.1073/pnas.1202894110.

Chambers, J.Q., Robertson, A.L., Carneiro, V.M., Lima, A.J., Smith, M.L., Plourde, L.C., Higuchi, N., 2009. Hyperspectral remote detection of niche partitioning among canopy trees driven by blowdown gap disturbances in the central amazon. Oecologia 160, 107–117. doi:10.1007/s00442-008-1274-9.

Chambers, J.Q., Tribuzy, E.S., Toledo, L.C., Crispim, B.F., Higuchi, N., Santos, J.d., Araújo, A.C., Kruijt, B., Nobre, A.D., Trumbore, S.E., 2004. Respiration from a tropical forest ecosystem: Partitioning of sources and low carbon use efficiency. Ecological Applications 14, 72–88. doi:10.1890/01-6012.

Chor, T.L., Dias, N.L., Araújo, A., Wolff, S., Zahn, E., Manzi, A., Trebs, I., Sá, M.O., Teixeira, P.R., Sörgel, M., 2017. Flux-variance and flux-gradient relationships in the roughness sublayer over the amazon forest. Agricultural and Forest Meteorology 239, 213–222. doi:10.1016/j.agrformet.2017.03.009.

Collow, A.B.M., Miller, M.A., 2016. The seasonal cycle of the radiation budget and cloud radiative effect in the amazon rain forest of brazil. Journal of Climate 29, 7703–7722. doi:10.1175/JCLI-D-16-0089.1.

Corrêa, P.B., Dias-Júnior, C.Q., Cava, D., Sörgel, M., Botía, S., Acevedo, O., Oliveira, P.E., Ocimar Manzi, A., Toledo Machado, L.A., dos Santos Martins, H., Tsokankunku, A., de Araújo, A.C., Lavric, J.V., Walter, D., Mortarini, L., 2021. A case study of a gravity wave induced by amazon forest orography and low level jet generation. Agricultural and Forest Meteorology 307, 108457. doi:https://doi.org/10.1016/j.agrformet.2021.108457.

Costa, F.D., Acevedo, O.C., Medeiros, L.E., Maroneze, R., Puhales, F.S., Jr., A.D.C., Camponogara, L.F., dos Santos, D.M., Mortarini, L., 2020. Stable boundary layer regimes in single-column models. Journal of the Atmospheric Sciences 77, 2039 – 2054. doi:10.1175/JAS-D-19-0218.1.

Dias-Júnior, C.Q., Dias, N.L., Fuentes, J.D., Chamecki, M., 2017a. Convective storms and non-classical low-level jets during high ozone level episodes in the amazon region: An arm/goamazon case study. Atmospheric Environment 155, 199–209. doi:10.1016/j.atmosenv.2017.02.006.

Dias-Júnior, C.Q., Sá, L.D., Marques Filho, E.P., Santana, R.A., Mauder, M., Manzi, A.O., 2017b. Turbulence regimes in the stable boundary layer above and within the amazon forest. Agricultural and Forest Meteorology 233, 122–132. doi:10.1016/j.agrformet.2016.11.001.

D'Oliveira, F.A., Cohen, J.C., Spracklen, D.V., Medeiros, A.S., Cirino, G.G., Artaxo, P., Dias-Júnior, C.Q., 2022. Simulation of the effects of biomass burning in a mesoscale convective system in the central amazon. Atmospheric Research 278, 106345.

Espírito-Santo, F.D., Gloor, M., Keller, M., Malhi, Y., Saatchi, S., Nelson, B., Junior, R.C.O., Pereira, C., Lloyd, J., Frolking, S., et al., 2014. Size and frequency of natural forest disturbances and the amazon forest carbon balance. Nature communications 5, 1–6. doi:10.1038/ncomms4434.

Feng, Y., Negrón-Juárez, R.I., Romps, D.M., Chambers, J.Q., 2023. Amazon windthrow disturbances are likely to increase with storm frequency under global warming. Nature Communications 14, 101. doi:10.1038/s41467-022-35570-1.

Finnigan, J., 2000. Turbulence in plant canopies. Annual Review of Fluid Mechanics 32, 519–571. doi:10.1146/annurev.fluid.32.1.519.

Freundorfer, A., Rehberg, I., Law, B.E., Thomas, C., 2019. Forest wind regimes and their implications on cross-canopy coupling. Agricultural and Forest Meteorology 279, 107696. doi:https://doi.org/10.1016/j.agrformet.2019.107696.

Fuentes, J.D., Chamecki, M., dos Santos, R.M.N., Randow, C.V., Stoy, P.C., Katul, G., Fitzjarrald, D., Manzi, A., Gerken, T., Trowbridge, A., Freire, L.S., Ruiz-Plancarte, J., Maia, J.M.F., Tóta, J., Dias, N., Fisch, G., Schumacher, C., Acevedo, O., Mercer, J.R., Yañez-Serrano, A.M., 2016. Linking meteorology, turbulence, and air chemistry in the amazon rain forest. Bulletin of the American Meteorological Society 97, 2329 – 2342. doi:10.1175/BAMS-D-15-00152.1.

Fujita, T., 1985. The downburst: Microburst and macroburst. Satellite and Mesometeorology Research Project, Department of the Geophysical Sciences, University of Chicago 210, 122.

Garstang, M., Fitzjarrald, D.R., 1999. Observations of surface to atmosphere interactions in the tropics. Oxford University Press, USA. doi:10.1016/S0168-1923(03)00003-0.

Garstang, M., White, S., Shugart, H., Halverson, J., 1998. Convective cloud downdrafts as the cause of large blowdowns in the amazon rainforest. Meteorology and Atmospheric Physics 67, 199–212. doi:10.1007/BF01277510.

Gerken, T., Wei, D., Chase, R.J., Fuentes, J.D., Schumacher, C., Machado, L.A., Andreoli, R.V., Chamecki, M., Ferreira de Souza, R.A., Freire, L.S., Jardine, A.B., Manzi, A.O., Nascimento dos Santos, R.M., von Randow, C., dos Santos Costa, P., Stoy, P.C., Tóta, J., Trowbridge, A.M., 2016. Downward transport of ozone rich air and implications for atmospheric chemistry in the amazon rainforest. Atmospheric Environment 124, 64–76. doi:10.1016/j.atmosenv.2015.11.014.

Greco, S., Ulanski, S., Garstang, M., Houston, S., 1992. Low-level nocturnal wind maximum over the central amazon basin. Boundary-layer meteorology 58, 91–115. doi:10.1007/BF00120753.

Guerra, V.S., Acevedo, O.C., Medeiros, L.E., Oliveira, P.E., Santos, D.M., 2018. Small-scale horizontal variability of mean and turbulent quantities in the nocturnal boundary layer. Boundary-Layer Meteorology 169, 395–411. doi:10.1007/s10546-018-0381-3.

Knohl, A., Baldocchi, D.D., 2008. Effects of diffuse radiation on canopy gas exchange processes in a forest ecosystem. Journal of Geophysical Research: Biogeosciences 113. doi:10.1029/2007JG000663.

Machado, L., Laurent, H., Dessay, N., Miranda, I., 2004. Seasonal and diurnal variability of convection over the amazonia: A comparison of different vegetation types and large scale forcing. Theoretical and Applied Climatology 78, 61–77. doi:10.1007/s00704-004-0044-9.

Machado, L.A.T., Laurent, H., Lima, A.A., 2002. Diurnal march of the convection observed during trmm-wetamc/lba. Journal of Geophysical Research: Atmospheres 107, LBA 31–1–LBA 31–15. doi:10.1029/2001JD000338.

Mahrt, L., 1998. Nocturnal boundary-layer regimes. Boundary-layer meteorology 88, 255–278.

Mahrt, L., 2014. Stably stratified atmospheric boundary layers. Annual Review of Fluid Mechanics 46, 23–45. doi:10.1146/annurev-fluid-010313-141354.

Mahrt, L., Thomas, C., Richardson, S., Seaman, N., Stauffer, D., Zeeman, M., 2013. Non-stationary generation of weak turbulence for very stable and weak-wind conditions. Boundary-layer meteorology 147, 179–199. doi:10.1007/s10546-012-9782-x.

Malhi, Y., Meir, P., Brown, S., 2002. Forests, carbon and global climate. Philosophical Transactions of the Royal Society of London. Series A: Mathematical, Physical and Engineering Sciences 360, 1567–1591. doi:10.1098/rsta.2002.1020.

Marques Filho, A.d.O., Dallarosa, R.G., Pachêco, V.B., 2005. Radiação solar e distribuição vertical de área foliar em floresta-reserva biológica do cuieiras zf2, manaus. Acta Amazonica 35, 427–436. doi:10.1590/S0044-59672005000400007.

Marra, D.M., Chambers, J.Q., Higuchi, N., Trumbore, S.E., Ribeiro, G.H.P.M., dos Santos, J., Negrón-Juárez, R.I., Reu, B., Wirth, C., 2014. Large-scale wind disturbances promote tree diversity in a central amazon forest. PLOS ONE 9, 1–16. doi:10.1371/journal.pone.0103711.

Marra, D.M., Trumbore, S.E., Higuchi, N., Ribeiro, G.H.P.M., Negrón-Juárez, R.I., Holzwarth, F., Rifai, S.W., dos Santos, J., Lima, A.J.N., Kinupp, V.F., Chambers, J.Q., Wirth, C., 2018. Windthrows control biomass patterns and functional composition of amazon forests. Global Change Biology 24, 5867–5881. doi:10.1111/gcb.14457.

Melo, A.M., Dias-Junior, C.Q., Cohen, J.C., Sá, L.D., Cattanio, J.H., Kuhn, P.A., 2019. Ozone transport and thermodynamics during the passage of squall line in central amazon. Atmospheric Environment 206, 132–143. doi:https://doi.org/10.1016/j.atmosenv.2019.02.018.

Miranda, F.O., Ramos, F.M., von Randow, C., Dias-Júnior, C.Q., Chamecki, M., Fuentes, J.D., Manzi, A.O., de Oliveira, M.E., de Souza, C.M., 2020. Detection of extreme phenomena in the stable boundary layer over the amazonian forest. Atmosphere 11. doi:10.3390/atmos11090952.

Negrón-Juárez, R.I., Chambers, J.Q., Guimaraes, G., Zeng, H., Raupp, C.F.M., Marra, D.M., Ribeiro, G.H.P.M., Saatchi, S.S., Nelson, B.W., Higuchi, N., 2010. Widespread amazon forest tree mortality from a single cross-basin squall line event. Geophysical Research Letters 37. doi:10.1029/2010GL043733.

Negrón-Juárez, R.I., Holm, J.A., Marra, D.M., Rifai, S.W., Riley, W.J., Chambers, J.Q., Koven, C.D., Knox, R.G., McGroddy, M.E., Vittorio, A.V.D., Urquiza-Muñoz, J., Tello-Espinoza, R., Muñoz, W.A., Ribeiro, G.H.P.M., Higuchi, N., 2018. Vulnerability of amazon forests to storm-driven tree mortality 13, 054021. doi:10.1088/1748-9326/aabe9f.

Negrón-Juárez, R.I., Jenkins, H.S., Raupp, C.F.M., Riley, W.J., Kueppers, L.M., Magnabosco Marra, D., Ribeiro, G.H.P.M., Monteiro, M.T.F., Candido, L.A., Chambers, J.Q., Higuchi, N., 2017. Windthrow variability in central amazonia. Atmosphere 8. doi:10.3390/atmos8020028.

Nelson, B.W., 1994. Natural forest disturbance and change in the brazilian amazon. Remote Sensing Reviews 10, 105–125. doi:10.1080/02757259409532239.

Oliveira, A.N.d., Amaral, I.L.d., Ramos, M.B.P., Nobre, A.D., Couto, L.B., Sahdo, R.M., 2008. Composição e diversidade florístico-estrutural de um hectare de floresta densa de terra firme na amazônia central, amazonas, brasil. Acta amazônica 38, 627–641. doi:10.1590/S0044-59672008000400005.

Peterson, C.J., Ribeiro, G.H.P.d.M., Negrón-Juárez, R., Marra, D.M., Chambers, J.Q., Higuchi, N., Lima, A., Cannon, J.B., 2019. Critical wind speeds suggest wind could be an important disturbance agent in Amazonian forests. Forestry: An International Journal of Forest Research 92, 444–459. doi:10.1093/forestry/cpz025.

Raupach, M., Finningan, J., Brunet, Y., 1996. Coherent eddies and turbulence in vegetation canopies; the mixing. layer analogy. Boundary-Layer Meteorology 78, 351–382.

Ribeiro, G., Chambers, J., Peterson, C., Trumbore, S., Magnabosco Marra, D., Wirth, C., Cannon, J., Négron-Juárez, R., Lima, A., de Paula, E., Santos, J., Higuchi, N., 2016. Mechanical vulnerability and resistance to snapping and uprooting for central amazon tree species. Forest Ecology and Management 380, 1–10. doi:10.1016/j.foreco.2016.08.039.

Santana, R.A., Dias-Júnior, C.Q., da Silva, J.T., Fuentes, J.D., do Vale, R.S., Alves, E.G., dos Santos, R.M.N., Manzi, A.O., 2018. Air turbulence characteristics at multiple sites in and above the amazon rainforest canopy. Agricultural and Forest Meteorology 260, 41–54. doi:10.1016/j.agrformet.2018.05.027.

Santos, D.M., Acevedo, O.C., Chamecki, M., Fuentes, J.D., Gerken, T., Stoy, P.C., 2016. Temporal scales of the nocturnal flow within and above a forest canopy in amazonia. Boundary-Layer Meteorology 161, 73–98. doi:10.1007/s10546-016-0158-5.

dos Santos, L.T., Magnabosco Marra, D., Trumbore, S., de Camargo, P.B., Negrón-Juárez, R.I., Lima, A.J.N., Ribeiro, G.H.P.M., dos Santos, J., Higuchi, N., 2016. Windthrows increase soil carbon stocks in a central amazon forest. Biogeosciences 13, 1299–1308. doi:10.5194/bg-13-1299-2016.

Schwartz, N.B., Uriarte, M., DeFries, R., Bedka, K.M., Fernandes, K., Gutiérrez-Vélez, V., Pinedo-Vasquez, M.A., 2017. Fragmentation increases wind disturbance impacts on forest structure and carbon stocks in a western amazonian landscape. Ecological Applications 27, 1901–1915. doi:10.1002/eap.1576.

Serra-Neto, E.M., Martins, H.S., Dias-Júnior, C.Q., Santana, R.A., Brondani, D.V., Manzi, A.O., de Araújo, A.C., Teixeira, P.R., Sörgel, M., Mortarini, L., 2021. Simulation of the scalar transport above and within the amazon forest canopy. Atmosphere 12, 1631. doi:10.3390/atmos12121631.

Silvério, D.V., Brando, P.M., Bustamante, M.M.C., Putz, F.E., Marra, D.M., Levick, S.R., Trumbore, S.E., 2019. Fire, fragmentation, and windstorms: A recipe for tropical forest degradation. Journal of Ecology 107, 656–667. doi:10.1111/1365-2745.13076.

Sun, J., Burns, S.P., Lenschow, D.H., Banta, R., Newsom, R., Coulter, R., Frasier, S., Ince, T., Nappo, C., Cuxart, J., et al., 2002. Intermittent turbulence associated with a density current passage in the stable boundary layer. Boundary-Layer Meteorology 105, 199–219. doi:10.1023/A:1019969131774.

Sun, J., Lenschow, D.H., LeMone, M.A., Mahrt, L., 2016. The role of large-coherent-eddy transport in the atmospheric surface layer based on cases-99 observations. Boundary-layer meteorology 160, 83–111. doi:10.1007/s10546-016-0134-0.

Sun, J., Mahrt, L., Banta, R.M., Pichugina, Y.L., 2012. Turbulence regimes and turbulence intermittency in the stable boundary layer during cases-99. Journal of Atmospheric Sciences 69, 338–351. doi:10.1175/JAS-D-11-082.1.

Sun, J., Takle, E.S., Acevedo, O.C., 2020. Understanding physical processes represented by the monin–obukhov bulk formula for momentum transfer. Boundary-Layer Meteorology 177, 69–95. doi:10.1007/s10546-020-00546-5.

Telles, E.d.C.C., de Camargo, P.B., Martinelli, L.A., Trumbore, S.E., da Costa, E.S., Santos, J., Higuchi, N., Oliveira Jr., R.C., 2003. Influence of soil texture on carbon dynamics and storage potential in tropical forest soils of amazonia. Global Biogeochemical Cycles 17. doi:10.1029/2002GB001953.

Thomas, C., Foken, T., 2007. Flux contribution of coherent structures and its implications for the exchange of energy and matter in a tall spruce canopy. Boundary-Layer Meteorology 123, 317–337. doi:10.1007/s10546-006-9144-7.

Thomas, C.K., Martin, J.G., Law, B.E., Davis, K., 2013. Toward biologically meaningful net carbon exchange estimates for tall, dense canopies: Multi-level eddy covariance observations and canopy coupling regimes in a mature douglas-fir forest in oregon. Agricultural and forest meteorology 173, 14–27. doi:10.1016/j.agrformet.2013.01.001.

Tóta, J., Fitzjarrald, D.R., da Silva Dias, M.A., 2012. Exchange of carbon between the atmosphere and the tropical amazon rainforest, in: Sudarshana, P., Nageswara-Rao, M., Soneji, J.R. (Eds.), Tropical Forests. IntechOpen, Rijeka. chapter 16. doi:10.5772/29716.

Urquiza Muñoz, J.D., Magnabosco Marra, D., Negrón-Juarez, R.I., Tello-Espinoza, R., Alegría-Muñoz, W., Pacheco-Gómez, T., Rifai, S.W., Chambers, J.Q., Jenkins, H.S., Brenning, A., Trumbore, S.E., 2021. Recovery of forest structure following large-scale windthrows in the northwestern amazon. Forests 12. doi:10.3390/f12060667.

Vickers, D., Göckede, M., Law, B., 2010. Uncertainty estimates for 1-h averaged turbulence fluxes of carbon dioxide, latent heat and sensible heat. Tellus B: Chemical and Physical Meteorology 62, 87–99. doi:10.1111/j.1600-0889.2009.00449.x.

Vickers, D., Mahrt, L., 1997. Quality control and flux sampling problems for tower and aircraft data. Journal of Atmospheric and Oceanic Technology

14, 512 – 526. doi:10.1175/1520-0426(1997)014<0512:QCAFSP>2.0.CO;2.

Vignon, E., van de Wiel, B.J.H., van Hooijdonk, I.G.S., Genthon, C., van der Linden, S.J.A., van Hooft, J.A., Baas, P., Maurel, W., Traullé, O., Casasanta, G., 2017. Stable boundary-layer regimes at dome c, antarctica: observation and analysis. Quarterly Journal of the Royal Meteorological Society 143, 1241–1253. doi:10.1002/qj.2998.

Viswanadham, Y., Molion, L., Manzi, A., Sá, L., Filho, V.S., André, R., Nogueira, J., Santos, R.d., 1990. Micrometeorological measurements in amazon forest during gte/able 2a mission. Journal of Geophysical Research: Atmospheres 95, 13669–13682. doi:10.1029/JD095iD09p13669.

Von Randow, C., Manzi, A.O., Kruijt, B., De Oliveira, P., Zanchi, F.B., Silva, R.d., Hodnett, M.G., Gash, J.H., Elbers, J.A., Cardoso, F.L., et al., 2004. Comparative measurements and seasonal variations in energy and carbon exchange over forest and pasture in south west amazonia. Theoretical and Applied Climatology 78, 5–26. doi:10.1007/s00704-004-0041-z.

Wakimoto, R., 2015. Mesoscale meteorology— microbursts .

Zahn, E., Chor, T., Dias, N., 2016. A simple methodology for quality control of micrometeorological datasets. Am J Environ Eng 6, 135–142. doi:10.5923/s.ajee.201601.20.